

AI in Medicine: Transforming the landscape of Tissue-based Diagnostics

Behzad Najafian, M.D.

Department of Laboratory Medicine & Pathology

Department of Medicine

University of Washington, Seattle, USA



Disclosures

Behzad Najafian, M.D.

Receives grant/research support from: Amicus Therapeutics

Is **NOT** a member of any Speakers Bureau

Is a member of the Advisory Board for: Sanofi, Amicus, Avrobio, 4DMT, Sangamo, Freeline, AceLink, Relay, CRISPR, ELOXX, SPARK, UNIQUE

Disclosure will be made when a product is discussed for an unapproved use.

This continuing education activity is provided by AffinityCE, The Lysosomal and Rare Disorders Research and Treatment Center (LDRTC), and CheckRare CE. AffinityCE, CheckRare CE and LDRTC staff, planners, and reviewers, have no relevant financial relationships with ineligible companies to disclose. AffinityCE adheres to the ACCME's Standards for Integrity and Independence in Accredited Continuing Education. Any individuals in a position to control the content of a CME activity, including faculty, planners, reviewers, or others, are required to disclose all relevant financial relationships with ineligible companies. All relevant financial relationships when present, have been mitigated by the peer review of content by non-conflicted reviewers prior to the commencement of the activity.

This activity has been supported by educational grants from commercial supporters. Please see the final program for a list of all supporters.

Learning OBJECTIVES

At the conclusion of this activity, participants will be able to:

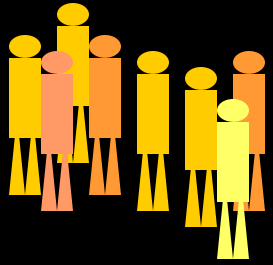
1. List some of the applications of AI in Pathology
2. Describe the importance of robust sampling in quantitative tissue analysis
3. Recognize the potentials of AI in standardization and accessibility of specialized tissue assays in rare diseases

University of Washington, Seattle

Worren Magnuson
Health Science Center

Najafian Lab →

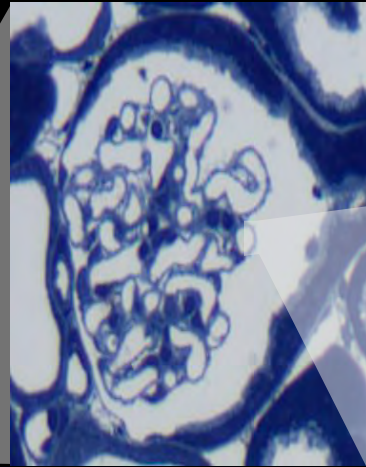




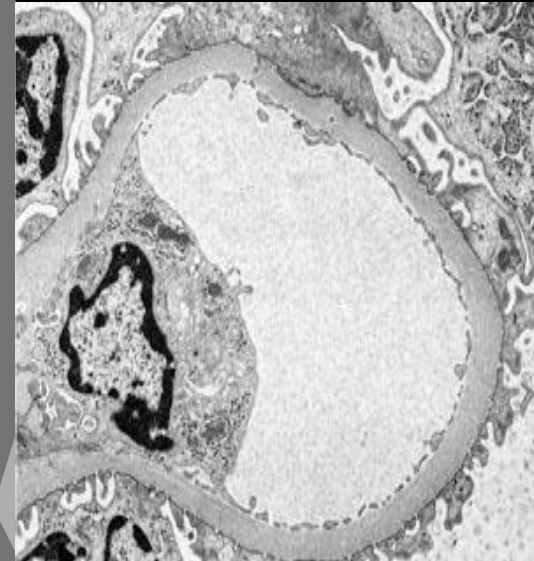
Biopsy
(1 cm)



400x



5,000x



60,000X



12,000x



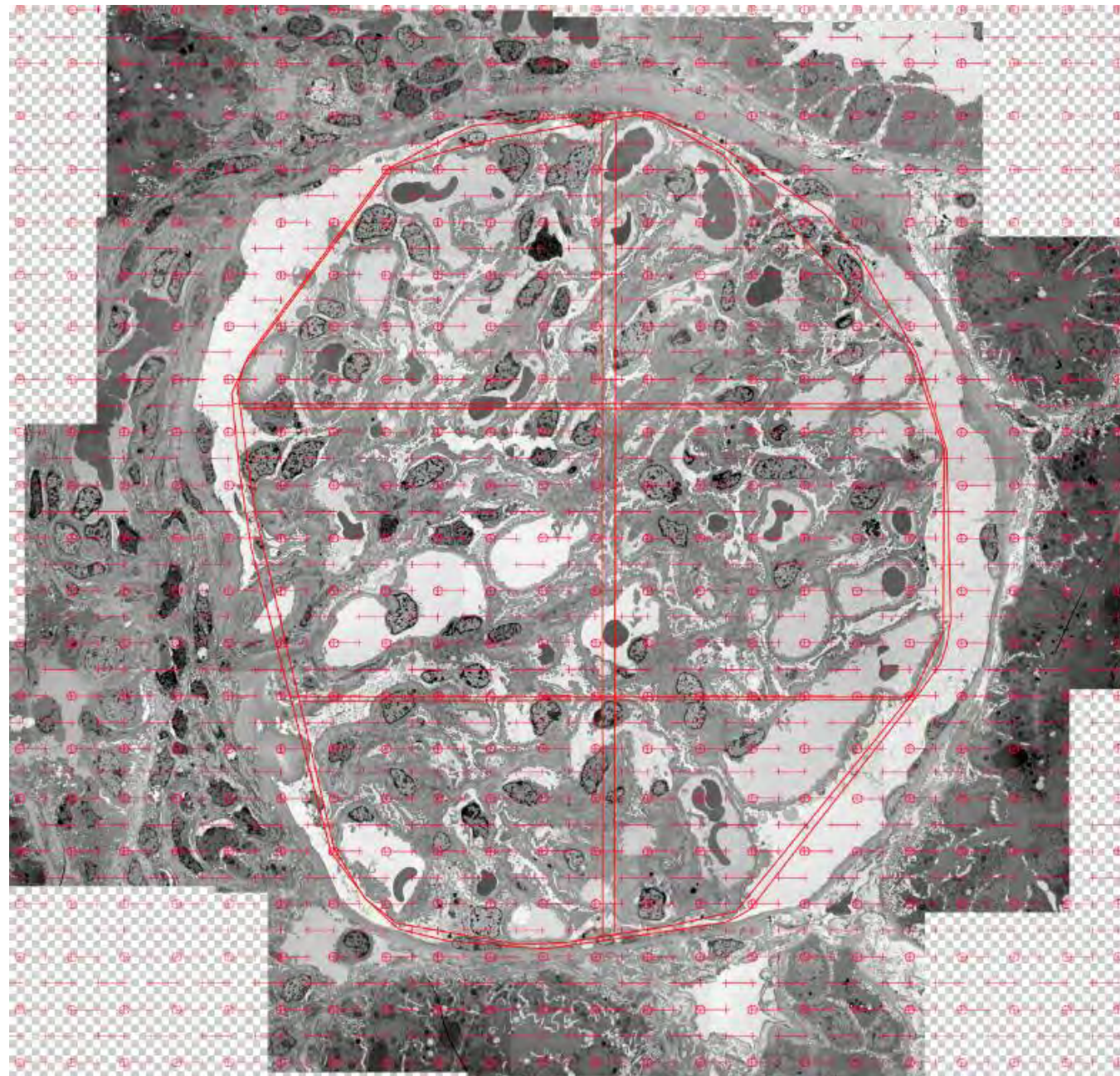
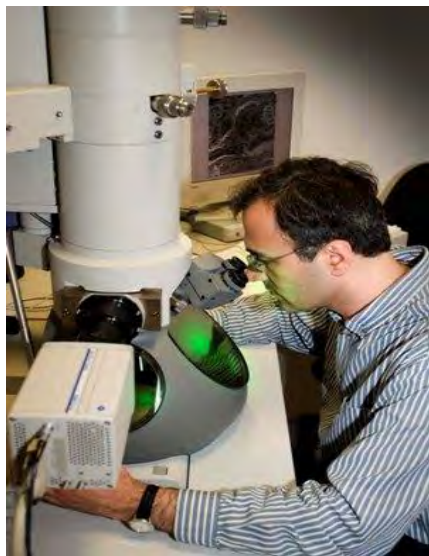
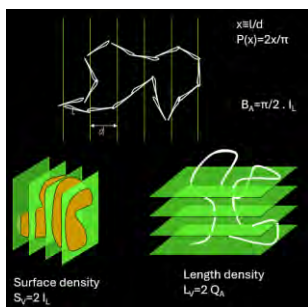
Lord Kelvin



I often say that when you can measure what you are speaking about, and express it in numbers, you know something about it; but when you cannot measure it, when you cannot express it in numbers, your knowledge is of a meagre and unsatisfactory kind.

AZ QUOTES

Stereology is a body of mathematical methods relating three-dimensional parameters defining the structure to two-dimensional measurements obtainable on sections of the structure.



Coefficient of error for line length	$CE(\hat{l}L) = \frac{\sqrt{VAR_{SRS}}}{\sum_{i=1}^n l_i}$
Variance of systematic random sampling (VAR_{SRS})	$VAR_{SRS} = \frac{3g_0 - 4g_1 + g_2}{12}$ $g_k = \sum_{i=1}^{n-k} L_i L_{i+k}$

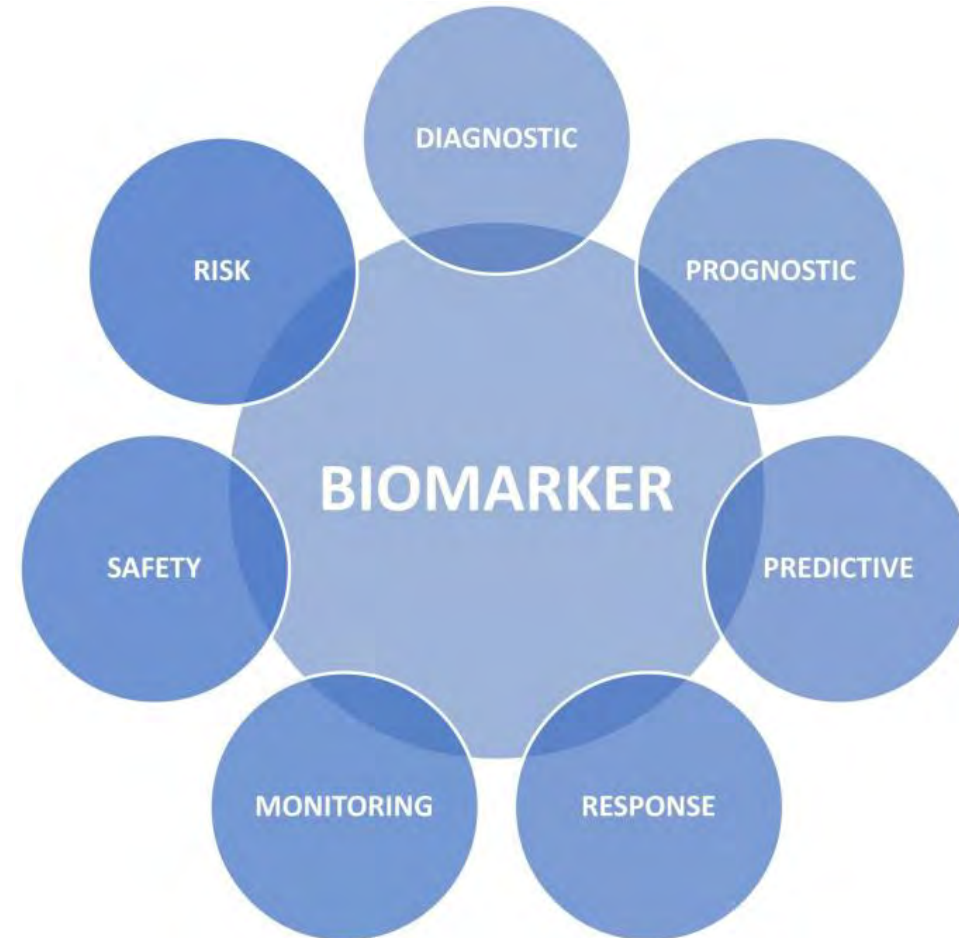
Biomarkers

Definition: A defined characteristic that is **measured (objectively)** as an indicator of normal biological processes, pathogenic processes, or biological responses to an exposure or intervention, including therapeutic interventions.

Biomarkers may include **molecular, histologic, radiographic,** or **physiologic** characteristics.

A biomarker **is not** a measure of how an individual feels, functions, or survives.

Biomarker categories according to the BEST resource (FDA)



Biomarker Categories

Susceptibility/risk biomarkers

Associated with the chance of developing a disease or condition

Diagnostic biomarkers

Confirms or establishes diagnosis.

Monitoring biomarker

Detects the change in degree or extent of disease.

Prognostic biomarker

Identifies the likelihood of a clinical event or progression
Enriches clinical trials with patients who have a higher likelihood of experiencing an event and therefore increase statistical power.

Predictive biomarker

Indicates the likelihood of benefiting from a treatment

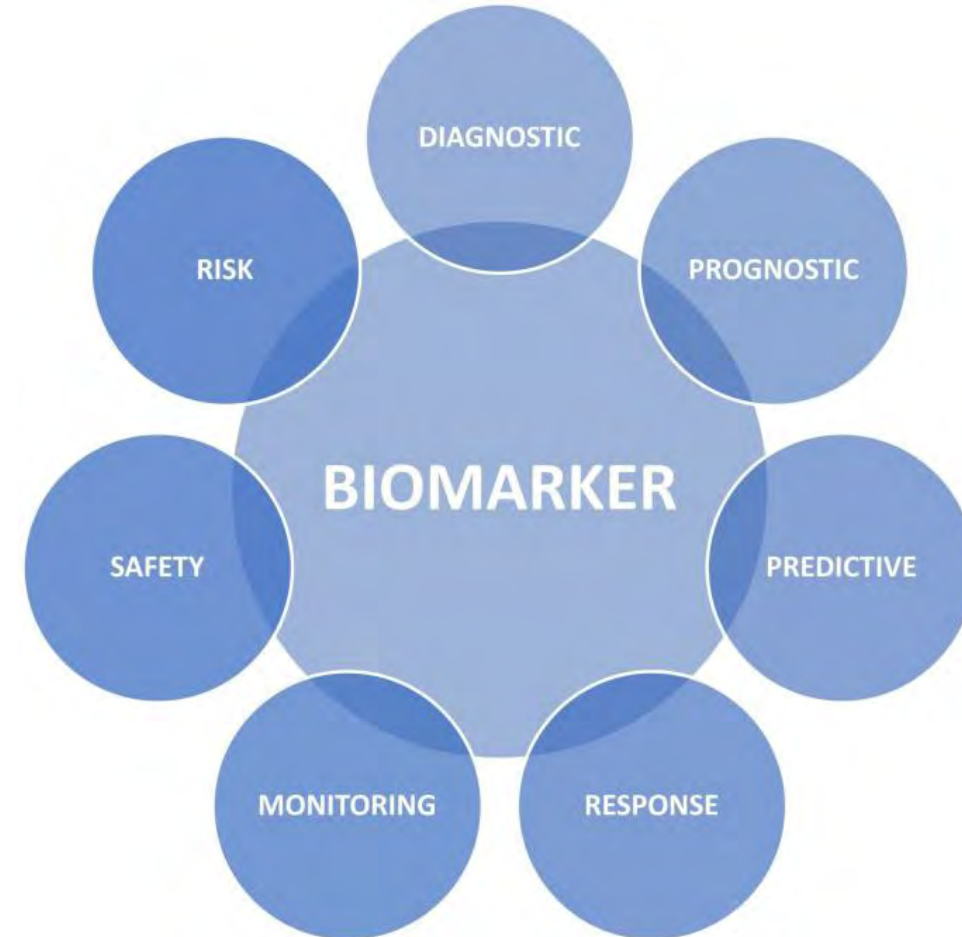
Pharmacodynamic (response) biomarker

Shows biological response to a treatment
May act as a surrogate clinical endpoint (also known as efficacy response biomarker) in a clinical trial when validated.

Safety biomarker

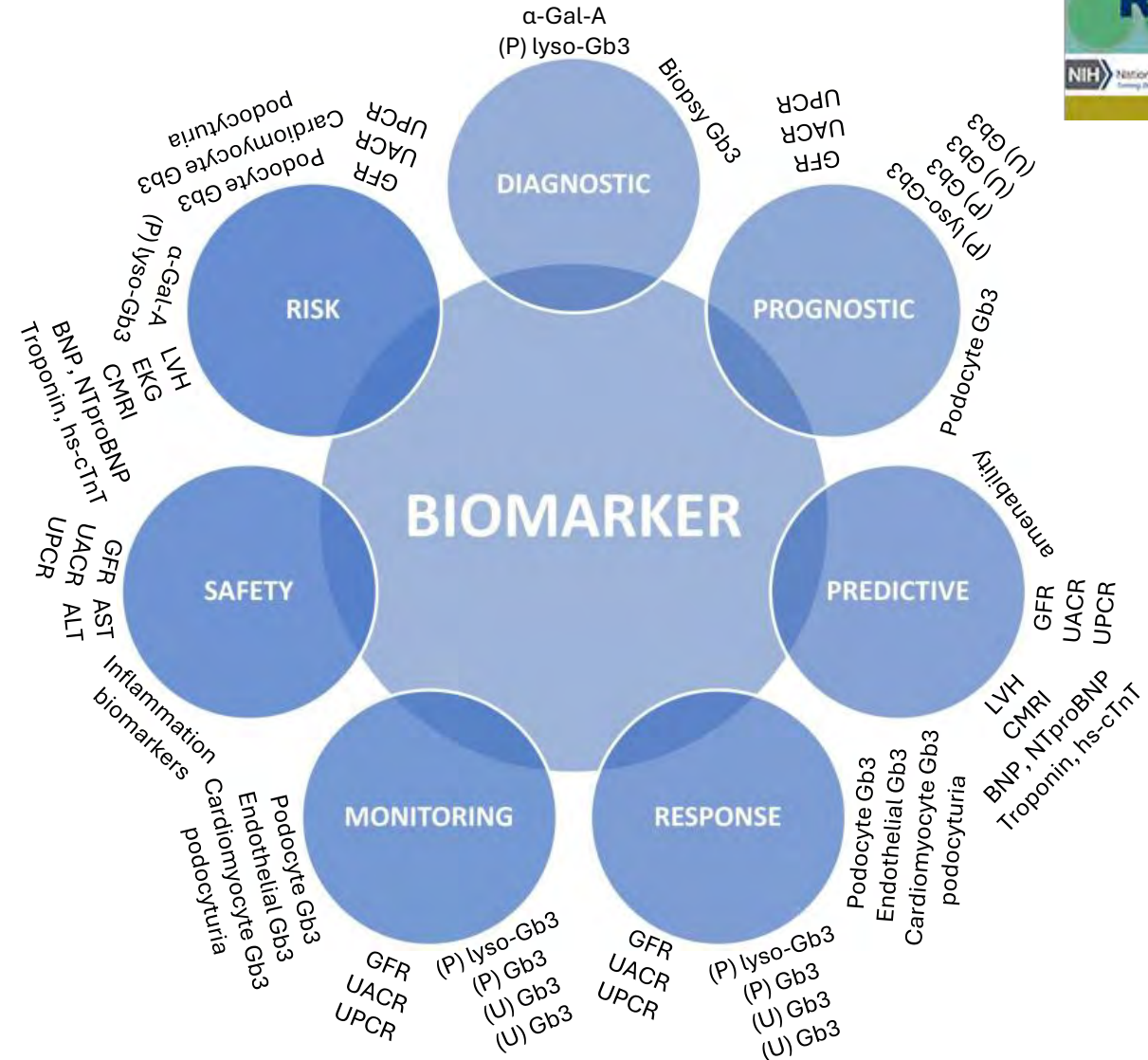
Monitors adverse effects of the therapy.

Biomarker categories according to the BEST resource (FDA)



Fabry Biomarker considerations

- It is critical to carefully specify the intention of use for a biomarker.
- A biomarker may report useful information on multiple categories, but may not be an ideal choice for all of them.
- Commonly we need multiple biomarkers for a given condition. Careful selection is the key. The more is not always the better.
- Biobanking, careful annotation, and democratic use of biospecimens are essential, especially when dealing with rare conditions.



Types of Biomarkers

Systemic Biomarkers: measurable indicators of a biological state or condition that reflects a broader, whole-body process, rather than being localized to a specific tissue or organ

- Plasma Gb3, plasma lyso-Gb3, plasma α -Gal-A activity, inflammatory biomarkers, etc.

Organ-specific Biomarkers: reflect the status of function, anatomy, or overall involvement of an organ by a disease or condition.

Non-invasive:

- Chemical:

Kidney: GFR, UACR, UPCR, urine Gb3 (?)

Heart: troponin, BNP, NT-proBNP

- Imaging:

Heart: LVH, CMRI, Non-contrast T-1 mapping,

Invasive (Biopsy):

Kidney: fibrosis, global glomerulosclerosis, kidney tissue Gb3

Heart: fibrosis, heart tissue Gb3

Cell-based Biomarkers: reflect the status of injury, function, accumulation, or morphology of specific cell types

Non-invasive:

- Chemical:

Heart: troponin, BNP, NT-proBNP, hs-cTnT, leukocyte α -Gal-A activity

- Microscopy, cytometry:

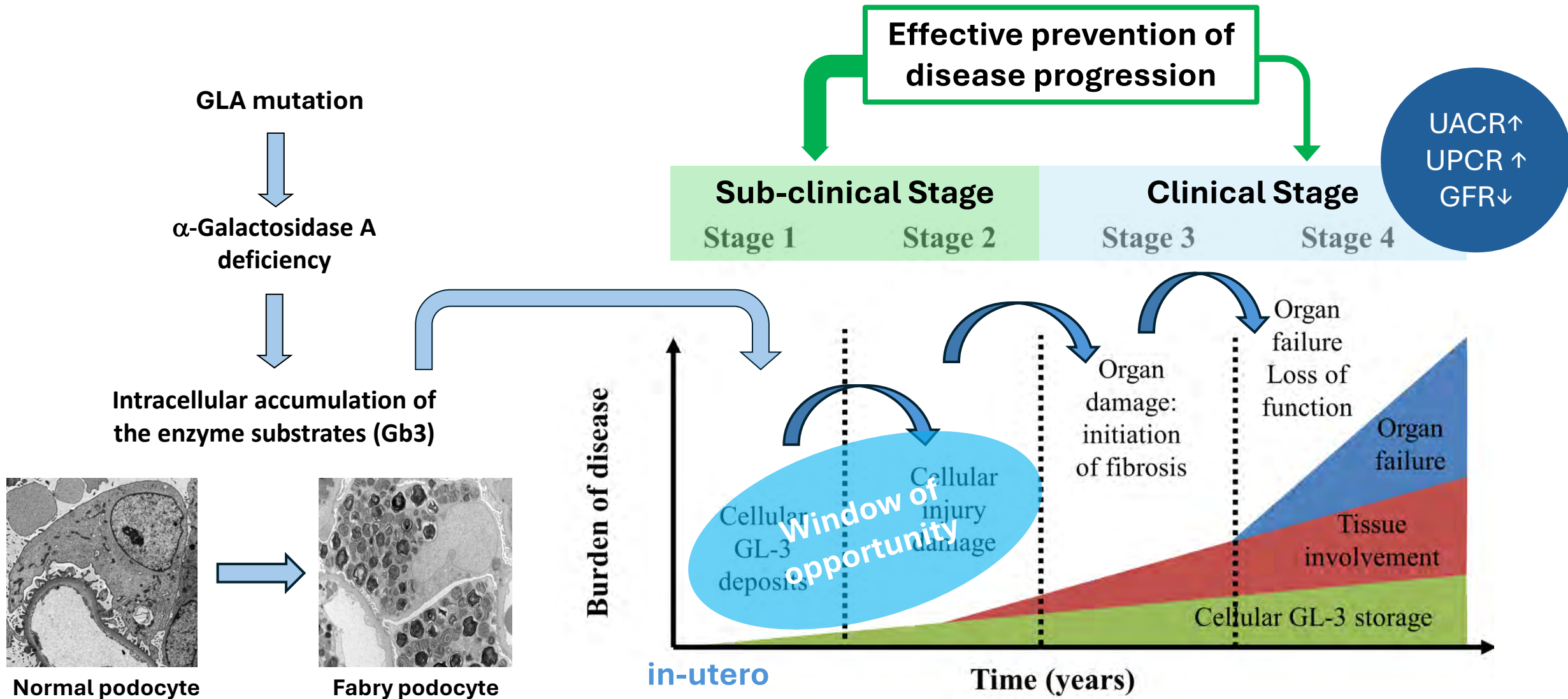
Kidney: podocyturia, podocyte Gb3, EVs

Invasive (Biopsy):

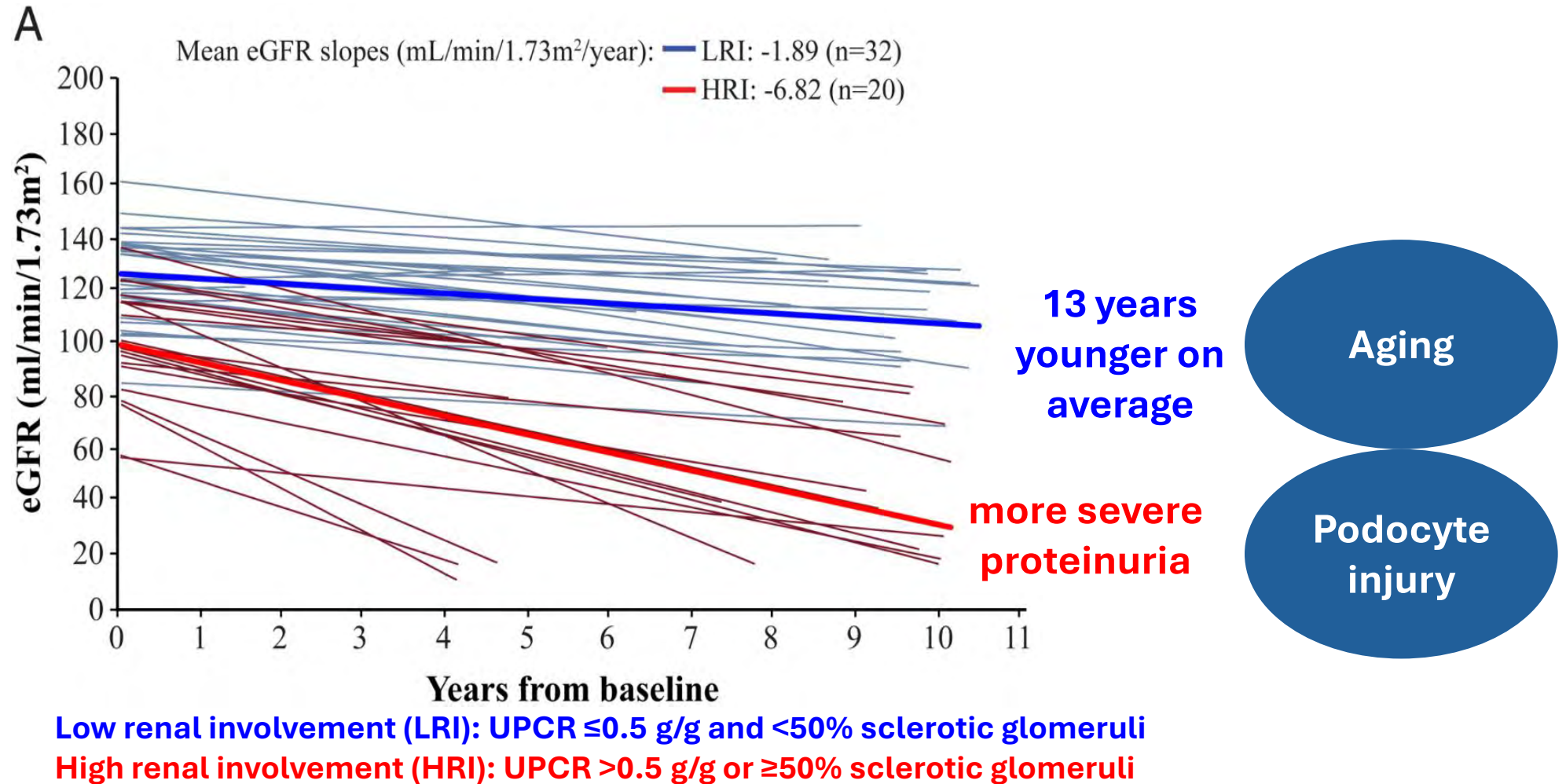
Kidney: Gb3 in various kidney cell types, podocyte number, podocyte foot process width

Heart: Gb3 in various cardiac cell types

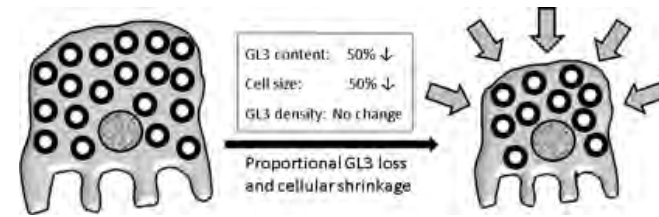
How does Fabry disease affect the kidneys?



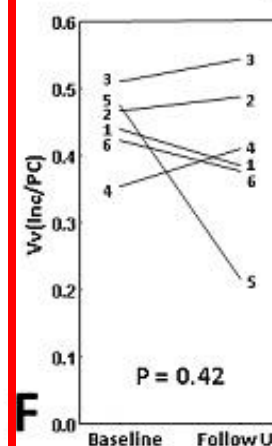
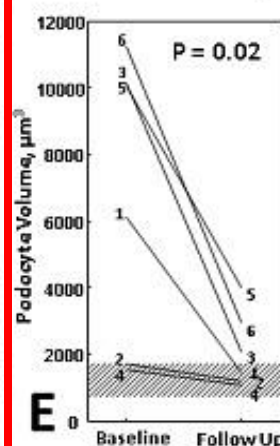
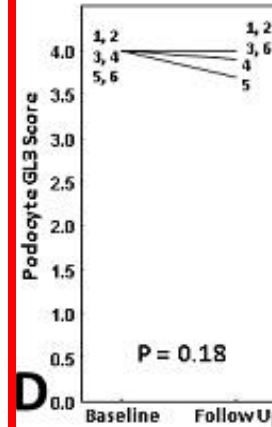
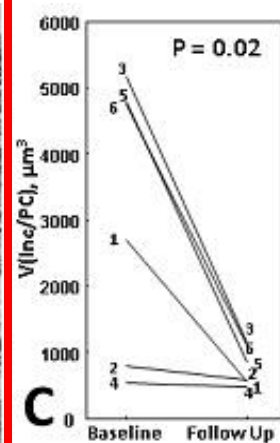
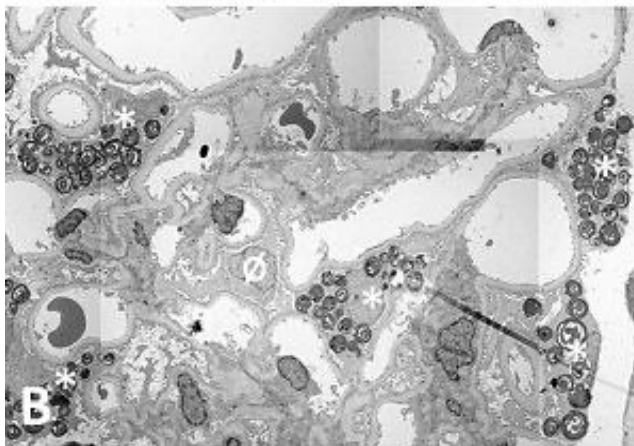
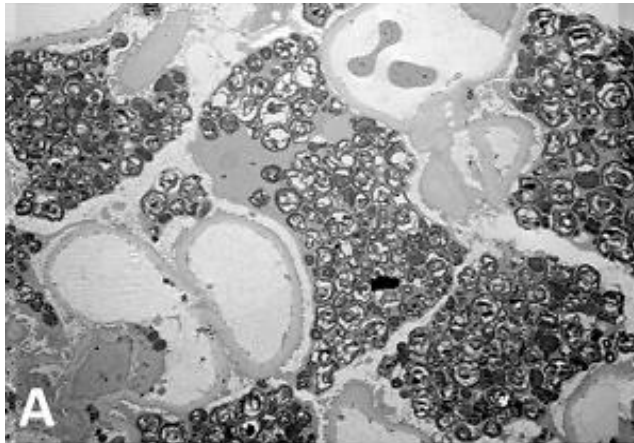
Late initiation of ERT may not stop progressive GFR loss in Fabry patients. This may at least in part be related to podocyte loss with age.



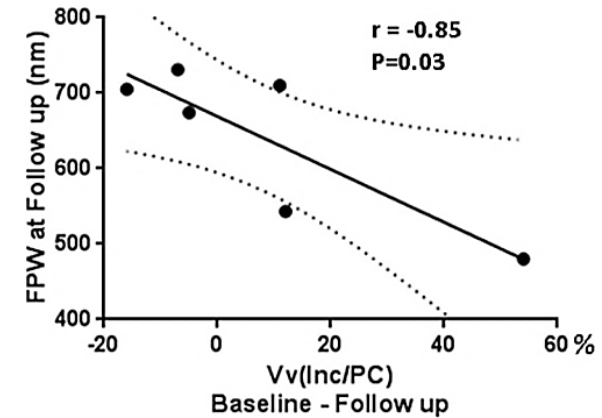
One Year of Enzyme Replacement Therapy Reduces Globotriaosylceramide Inclusions in Podocytes in Male Adult Patients with Fabry Disease



Behzad Najafian^{1*}, Camilla Tøndel^{2,3}, Einar Svarstad^{2,4}, Alexey Sokolovkiy¹, Kelly Smith¹, Michael Mauer⁵

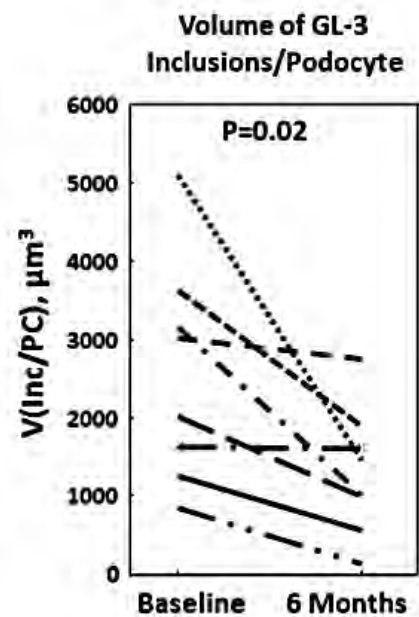


Reduction in GL-3 density in podocytes inversely correlated with foot process width at follow up

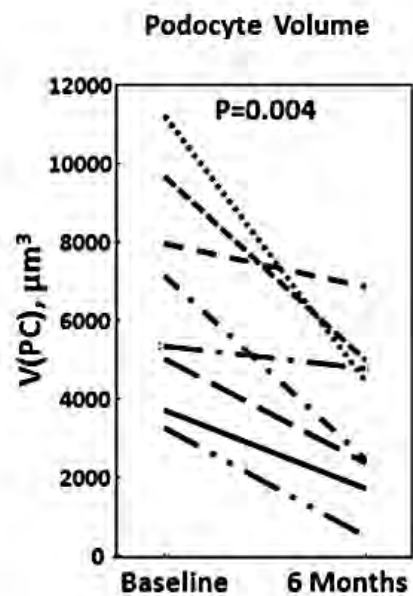


Reduction of podocyte globotriaosylceramide content in adult male patients with Fabry disease with amenable *GLA* mutations following 6 months of migalastat treatment

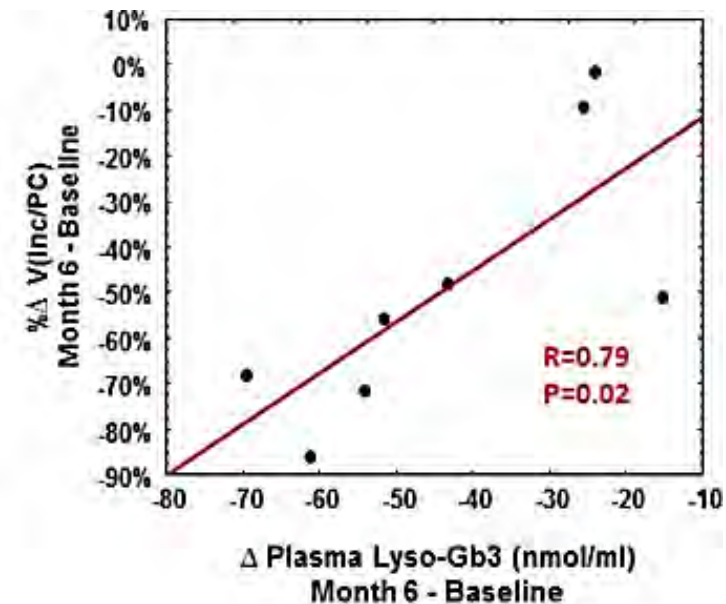
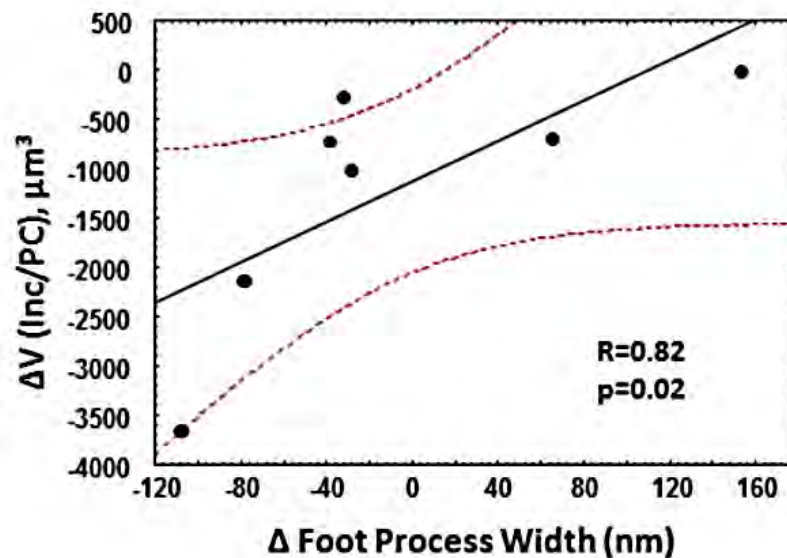
- Total volume of GL3 inclusions was reduced in podocytes after 6 months.
- Podocytes became smaller and foot process widening was improved parallel to GL3 clearance.



B



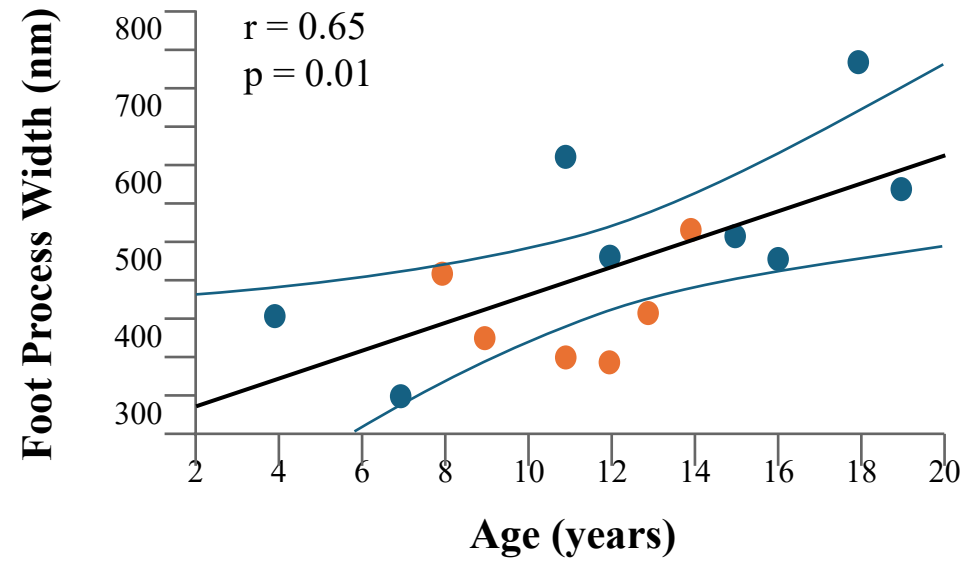
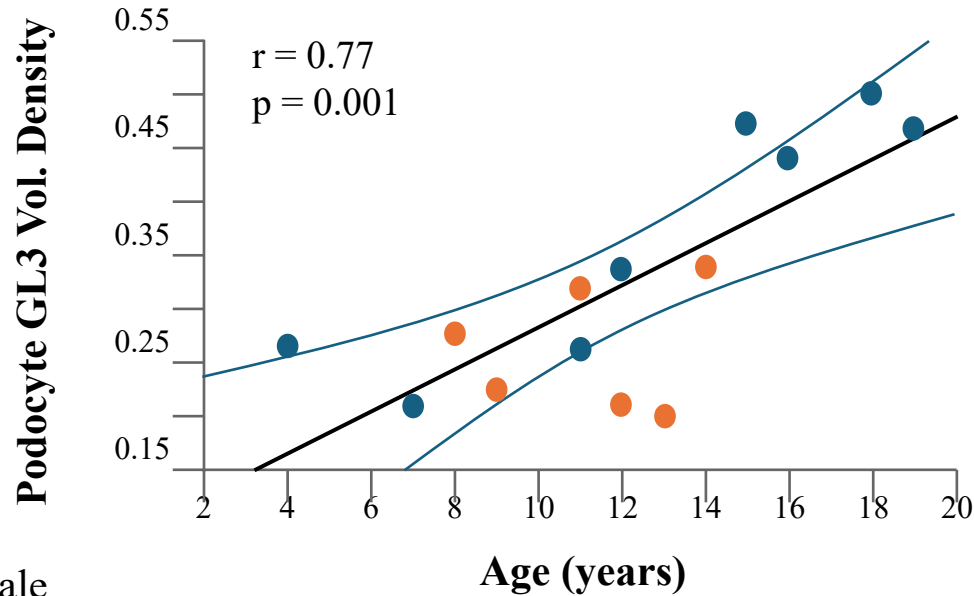
C



Progressive podocyte injury and globotriaosylceramide (GL-3) accumulation in young patients with Fabry disease

Behzad Najafian¹, Einar Svarstad^{2,3}, Leif Bostad^{4,5}, Marie-Claire Gubler⁶, Camilla Tøndel^{3,7}, Chester Whitley⁸ and Michael Mauer^{8,9}

Age < 20 years



● Male
● Female

Podocyte GL3 volume density and foot process width progressively increase with age in young Fabry patients with normal GFR and normal albuminuria

FPW, foot process width; Vv (Inc/EC), GL-3 inclusion fractional volume per endothelial cell; Vv (Inc/MC), GL-3 inclusion fractional volume per mesothelial cell; Vv(INC/PC), GL-3 inclusion fractional volume per podocyte cytoplasm

2024 Nobel Prize

2024 Nobel Prize in physics awarded to John J. Hopfield, Geoffrey E. Hinton for discoveries that 'enable machine learning with artificial neural networks'



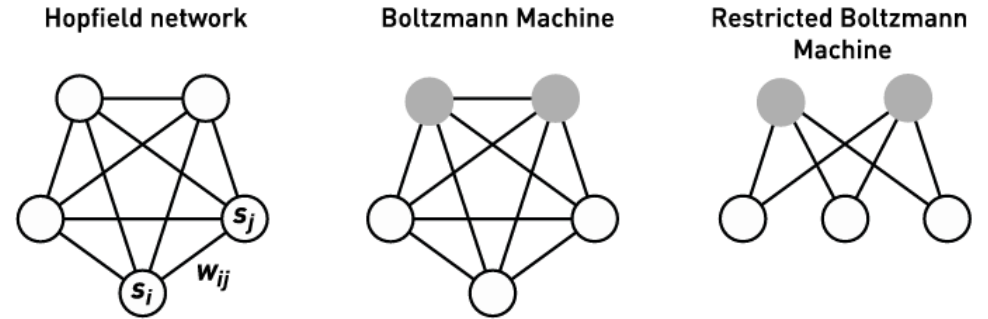
John J. Hopfield



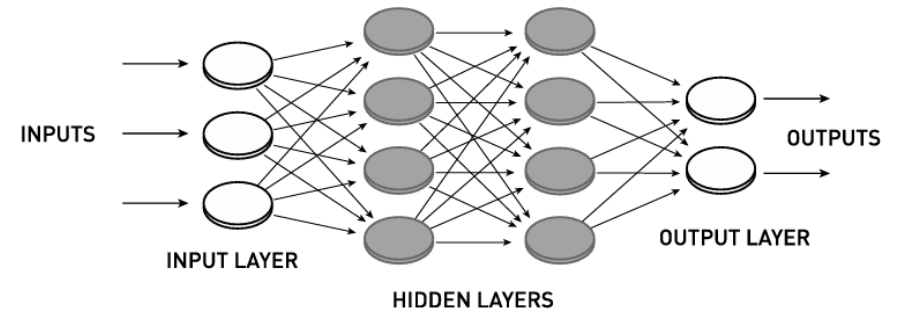
Geoffrey E. Hinton



In 1982, Hopfield published a dynamical model for an associative memory based on a simple recurrent neural network



In 1983–1985 Geoffrey Hinton, together with Terrence Sejnowski and other coworkers, developed a stochastic extension of Hopfield's model from 1982, called the Boltzmann machine



THE NOBEL PRIZE IN CHEMISTRY 2024



David
Baker

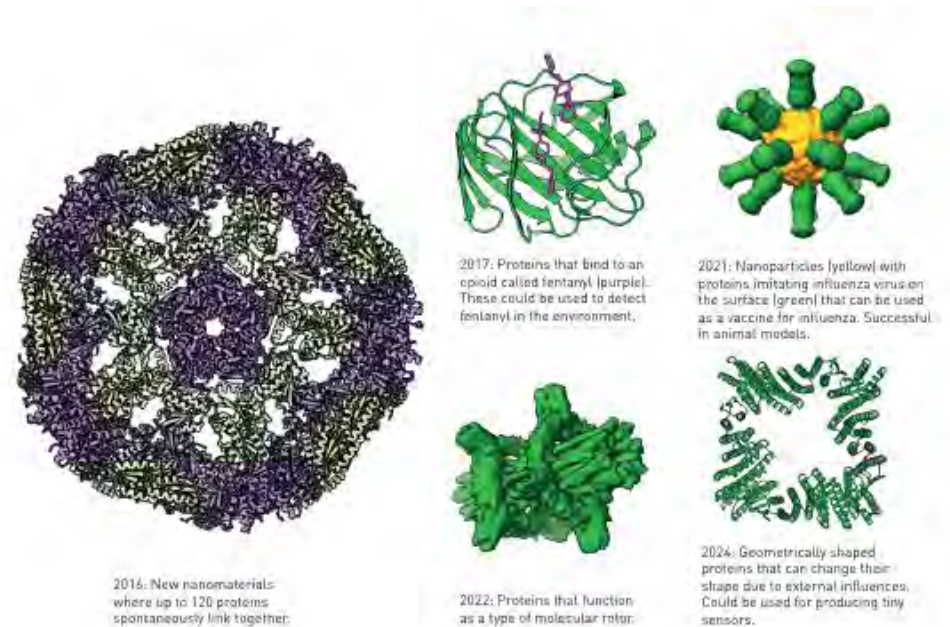
"for computational
protein design"

Demis
Hassabis

"for protein structure prediction"

John M.
Jumper

The Nobel Prize in Chemistry 2024 is about proteins, life's ingenious chemical tools. David Baker has succeeded with the almost impossible feat of building entirely new kinds of proteins. Demis Hassabis and John Jumper have developed an AI model to solve a 50-year-old problem: predicting proteins' complex structures. These discoveries hold enormous potential.



The AI Scientist: Towards Fully Automated Open-Ended Scientific Discovery

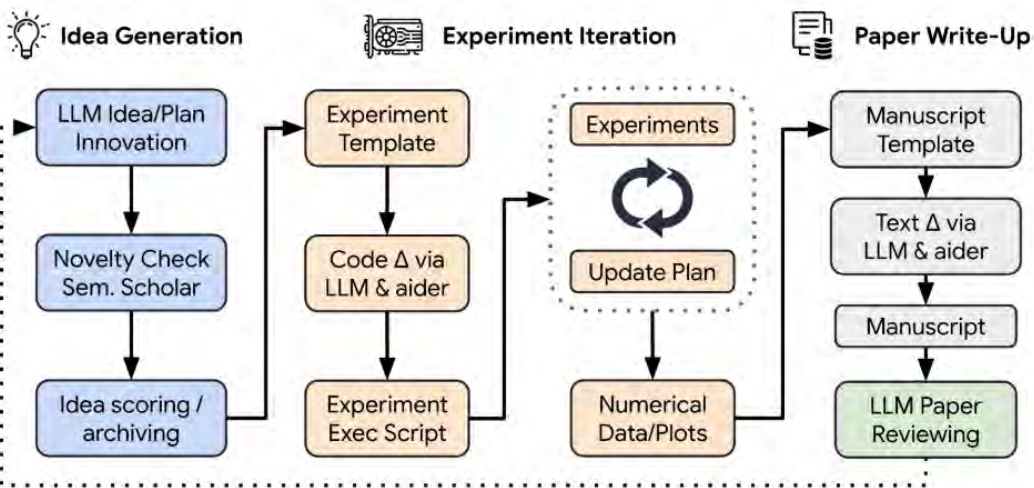
Chris Lu^{1,2,*}, Cong Lu^{3,4,*}, Robert Tjarko Lange^{1,*}, Jakob Foerster^{2,†}, Jeff Clune^{3,4,5,†} and David Ha^{1,†}

^{*}Equal Contribution, ¹Sakana AI, ²FLAIR, University of Oxford, ³University of British Columbia, ⁴Vector Institute, ⁵Canada CIFAR AI Chair, [†]Equal Advising

We developed methods to automatically merge the knowledge of multiple LLMs. In more recent work, we harnessed LLMs to discover new objective functions for tuning other LLMs.

This led us to dream even bigger: Can we use foundation models to automate the entire process of research itself?

Conceptual illustration of The AI Scientist.



<https://github.com/SakanaAI/AI-Scientist>

Examples of papers that were entirely autonomously generated by The AI Scientist.

AI-Scientist Generated Preprint

DUALSCALE DIFFUSION: ADAPTIVE FEATURE BALANCING FOR LOW-DIMENSIONAL GENERATIVE MODELS

Anonymous authors
Paper under double-blind review

ABSTRACT

This paper introduces an adaptive dual-scale denoising approach for low-dimensional diffusion models, addressing the challenge of balancing global structure and local detail in generated samples. While diffusion models have shown remarkable success in high-dimensional spaces, their application to low-dimensional data remains crucial for understanding fundamental model behaviors and addressing real-world applications with inherently low-dimensional data. However, in these spaces, traditional models often struggle to simultaneously capture both macro-level patterns and fine-grained features, leading to suboptimal sample quality. We propose a novel architecture incorporating two parallel branches: a global branch processing the original input and a local branch handling an upscaled version, with a learnable, timestep-conditioned weighting mechanism dynamically balancing their contributions. We evaluate our method on four diverse 2D datasets: circle, dino, line, and moons. Our results demonstrate significant improvements in sample quality, with KL divergence reductions of up to 12.8% compared to the baseline model. The adaptive weighting successfully adjusts the focus between global and local features across different datasets and denoising stages, as evidenced by our weight evolution analysis. This work not only enhances low-dimensional diffusion models but also provides insights that could inform improvements in higher-dimensional domains, opening new avenues for advancing generative modeling across various applications.

1 INTRODUCTION

Diffusion models have emerged as a powerful class of generative models, achieving state-of-the-art results in a wide range of tasks, including image synthesis, audio generation, and text-to-image synthesis. The key challenge in these models is balancing global structure and local detail in generated samples. While diffusion models have shown remarkable success in high-dimensional spaces, their application to low-dimensional data remains crucial for understanding fundamental model behaviors and addressing real-world applications with inherently low-dimensional data. However, in these spaces, traditional models often struggle to simultaneously capture both macro-level patterns and fine-grained features, leading to suboptimal sample quality. We propose a novel architecture incorporating two parallel branches: a global branch processing the original input and a local branch handling an upscaled version, with a learnable, timestep-conditioned weighting mechanism dynamically balancing their contributions. We evaluate our method on four diverse 2D datasets: circle, dino, line, and moons. Our results demonstrate significant improvements in sample quality, with KL divergence reductions of up to 12.8% compared to the baseline model. The adaptive weighting successfully adjusts the focus between global and local features across different datasets and denoising stages, as evidenced by our weight evolution analysis. This work not only enhances low-dimensional diffusion models but also provides insights that could inform improvements in higher-dimensional domains, opening new avenues for advancing generative modeling across various applications.

AI-Scientist Generated Preprint

REINFORCED LEARNING IN LOW-DIMENSIONAL EXPERTS

Anonymous authors
Paper under double-blind review

ABSTRACT

Reinforced learning in low-dimensional spaces is a challenging task due to the limited number of states and actions. This paper introduces a novel approach to this problem by leveraging the power of diffusion models. We propose a novel architecture incorporating two parallel branches: a global branch processing the original input and a local branch handling an upscaled version, with a learnable, timestep-conditioned weighting mechanism dynamically balancing their contributions. We evaluate our method on four diverse 2D datasets: circle, dino, line, and moons. Our results demonstrate significant improvements in sample quality, with KL divergence reductions of up to 12.8% compared to the baseline model. The adaptive weighting successfully adjusts the focus between global and local features across different datasets and denoising stages, as evidenced by our weight evolution analysis. This work not only enhances low-dimensional diffusion models but also provides insights that could inform improvements in higher-dimensional domains, opening new avenues for advancing generative modeling across various applications.

1 INTRODUCTION

Reinforced learning in low-dimensional spaces is a challenging task due to the limited number of states and actions. This paper introduces a novel approach to this problem by leveraging the power of diffusion models. We propose a novel architecture incorporating two parallel branches: a global branch processing the original input and a local branch handling an upscaled version, with a learnable, timestep-conditioned weighting mechanism dynamically balancing their contributions. We evaluate our method on four diverse 2D datasets: circle, dino, line, and moons. Our results demonstrate significant improvements in sample quality, with KL divergence reductions of up to 12.8% compared to the baseline model. The adaptive weighting successfully adjusts the focus between global and local features across different datasets and denoising stages, as evidenced by our weight evolution analysis. This work not only enhances low-dimensional diffusion models but also provides insights that could inform improvements in higher-dimensional domains, opening new avenues for advancing generative modeling across various applications.

AI-Scientist Generated Preprint

GAN-ENHANCED DIFFUSION: IMPROVING QUALITY AND DIVERSITY

Anonymous authors
Paper under double-blind review

ABSTRACT

Generative models have become a powerful tool for creating high-quality and diverse samples. However, in these spaces, traditional models often struggle to simultaneously capture both macro-level patterns and fine-grained features, leading to suboptimal sample quality. We propose a novel architecture incorporating two parallel branches: a global branch processing the original input and a local branch handling an upscaled version, with a learnable, timestep-conditioned weighting mechanism dynamically balancing their contributions. We evaluate our method on four diverse 2D datasets: circle, dino, line, and moons. Our results demonstrate significant improvements in sample quality, with KL divergence reductions of up to 12.8% compared to the baseline model. The adaptive weighting successfully adjusts the focus between global and local features across different datasets and denoising stages, as evidenced by our weight evolution analysis. This work not only enhances low-dimensional diffusion models but also provides insights that could inform improvements in higher-dimensional domains, opening new avenues for advancing generative modeling across various applications.

1 INTRODUCTION

Generative models have become a powerful tool for creating high-quality and diverse samples. However, in these spaces, traditional models often struggle to simultaneously capture both macro-level patterns and fine-grained features, leading to suboptimal sample quality. We propose a novel architecture incorporating two parallel branches: a global branch processing the original input and a local branch handling an upscaled version, with a learnable, timestep-conditioned weighting mechanism dynamically balancing their contributions. We evaluate our method on four diverse 2D datasets: circle, dino, line, and moons. Our results demonstrate significant improvements in sample quality, with KL divergence reductions of up to 12.8% compared to the baseline model. The adaptive weighting successfully adjusts the focus between global and local features across different datasets and denoising stages, as evidenced by our weight evolution analysis. This work not only enhances low-dimensional diffusion models but also provides insights that could inform improvements in higher-dimensional domains, opening new avenues for advancing generative modeling across various applications.

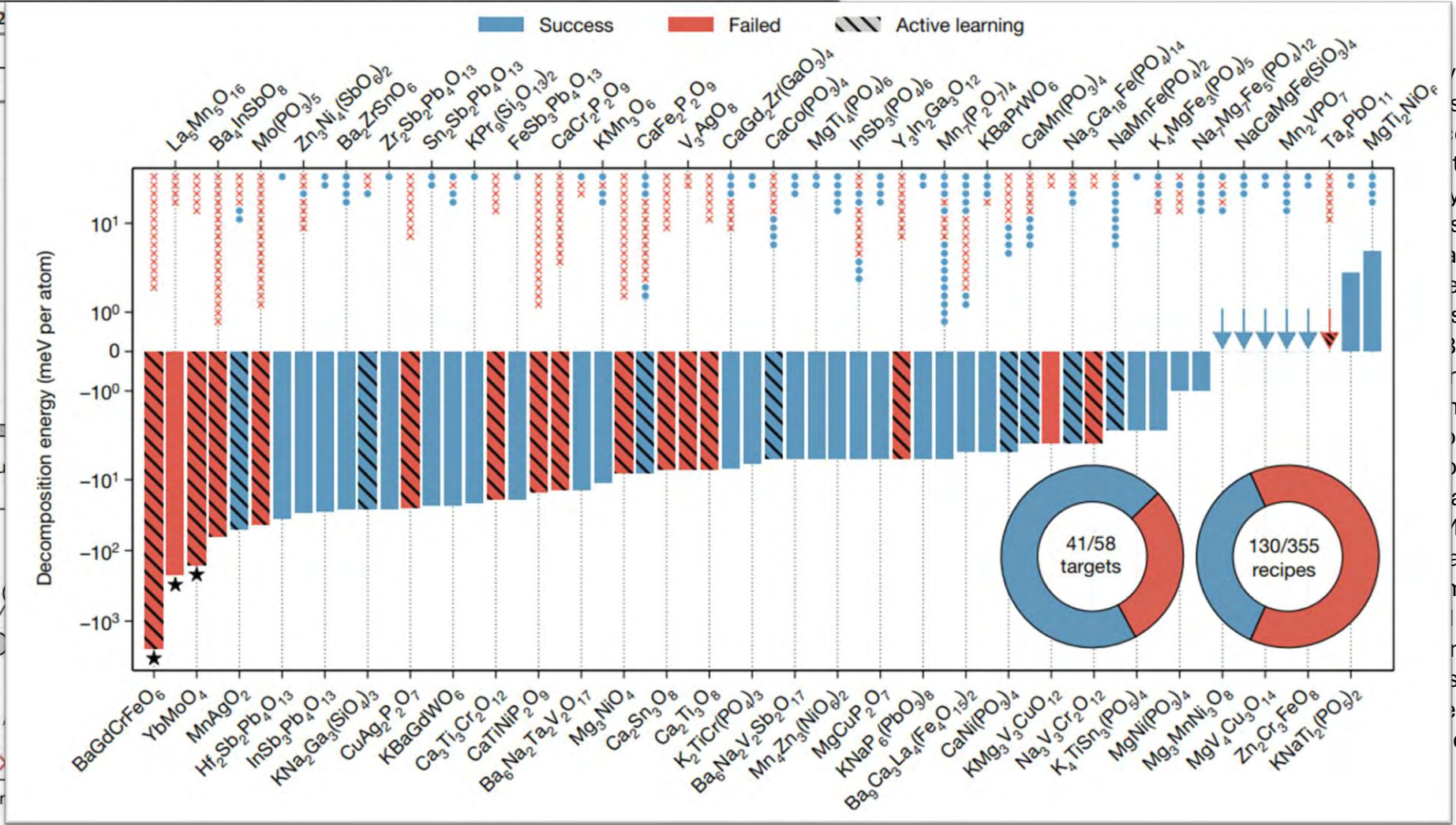
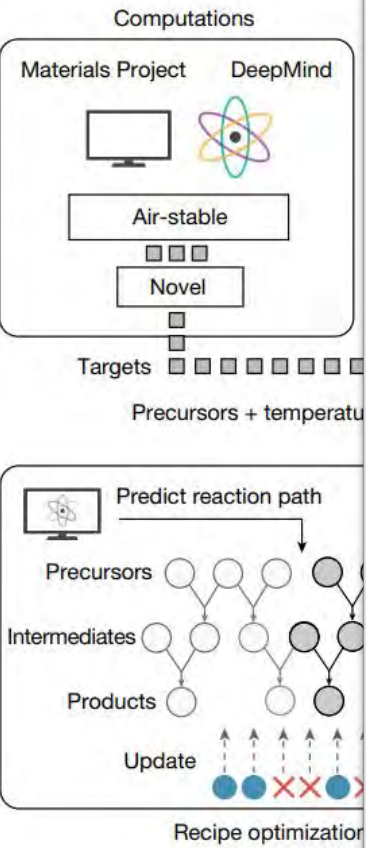
An autonomous laboratory for the accelerated synthesis of novel materials

In 17 days of closed-loop operation, the A-Lab performed 355 experiments and successfully realized 41 of 58 (71%) novel inorganic crystalline solids with diverse structures and chemistries.

<https://doi.org/10.1038/s41586-023>

Received: 16 May 2023

Accepted: 10 October 2023



with the A-
s are
convex hulls
the Materials
synthesis
sed using ML
a from the
ed using a
s (1) powder
3) product
mple transfer
med using
omated
o
assessed
ML models
aterials
med with
n cases in
not obtained,
sed by an
entifies
driving force



ILLUSTRATION: ARIHA YOKA

WILL AI EVER WIN ITS OWN NOBEL PRIZE?

Some researchers predict a science breakthrough by 2050. Others are sceptical. **By Jenna Ahart**

Arificial intelligence models are starting to succeed in science. In the past two years, they have demonstrated that they can analyse data, design experiments and even come up with new hypotheses. The pace of progress has some researchers convinced that artificial intelligence (AI) could compete with science's greatest minds in the next few decades.

In 2016, Hiroaki Kitano, a biologist and chief executive at Sony AI, challenged researchers to accomplish just that: to develop an AI system so advanced that it could make a discovery worthy of a Nobel prize. Calling it the Nobel Turing Challenge, Kitano presented the endeavour as the grand challenge for AI in science¹. A machine wins if it can achieve a discovery on a par with top-level human research.

That's not something current models can do. But by 2050, the Nobel Turing Challenge envisions an AI system that, without human intervention, combines the skills of hypothesis generation, experimental planning and data analysis to make a breakthrough worthy of a Nobel prize.

PERSPECTIVE OPEN

Check for updates

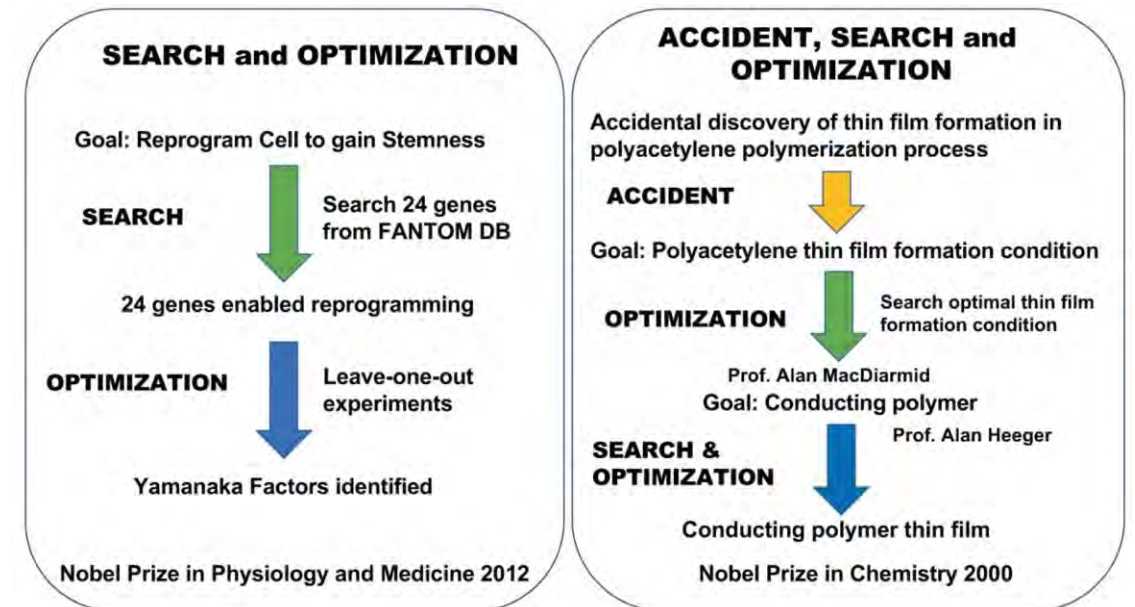
Nobel Turing Challenge: creating the engine for scientific discovery

Hiroaki Kitano ¹



Hiroaki Kitano
SONY CTO, Exec.
Deputy President

I propose the Nobel Turing Challenge as a grand challenge for artificial intelligence that aims at “developing AI Scientists capable of autonomously carrying out research to make major scientific discoveries and win a Nobel Prize by 2050”



Albania appoints world's first AI government 'minister' to root out corruption



The digital assistant, called Diella, is pictured as a woman dressed in traditional Albanian garb.

Albania has appointed the world's first artificial intelligence-generated government "minister", aiming to make the country "corruption-free".

The digital assistant is called Diella, meaning Sun, and has been advising people how to navigate government services online since January. On Thursday, Albania's Prime Minister Edi Rama announced the digital minister to his cabinet.

"Diella is the first [government] member who is not physically present, but virtually created by artificial intelligence," Rama said.

Diella will be entrusted with all decisions on public tenders, making them "100 per cent corruption-free," he said, adding that "every public fund submitted to the tender procedure will be perfectly transparent".

Next Tech News

Albania's AI minister is 'pregnant' with 83 digital assistants, prime minister says



Copyright AP Photo/Vlasov Sulaj

By Euronews

Published on 30/10/2025 - 12:14 GMT+1

Share Comments

Diella, the country's first AI system that is now a minister in Edi Rama's cabinet, will have 83 "children," who will become parliamentary assistants.

Albania's first non-human minister made up entirely by artificial intelligence (AI) is "pregnant" with 83 children that will become parliamentary assistants, according to the country's prime minister.

Albanian Prime Minister Edi Rama told the Global Dialogue Forum in Berlin that the parliamentary assistants will participate in parliamentary sessions, keep notes on what goes on and then give advice to members on how they should react to specific pieces of legislation.

"These children will have their mother's knowledge regarding EU legislation and everything else," Rama said.

PERSPECTIVE

Tech's Love Affair with Trump Grows Stronger By the Day



PAUL M. BARRETT / OCT 23, 2025



President Donald Trump and First Lady Melania Trump host business and technology leaders for a dinner in State Dining Room at the White House, Thursday, September 4, 2025. (Official White House [photo](#) by Andrea Hanks)

The Exponential History of AI-ML

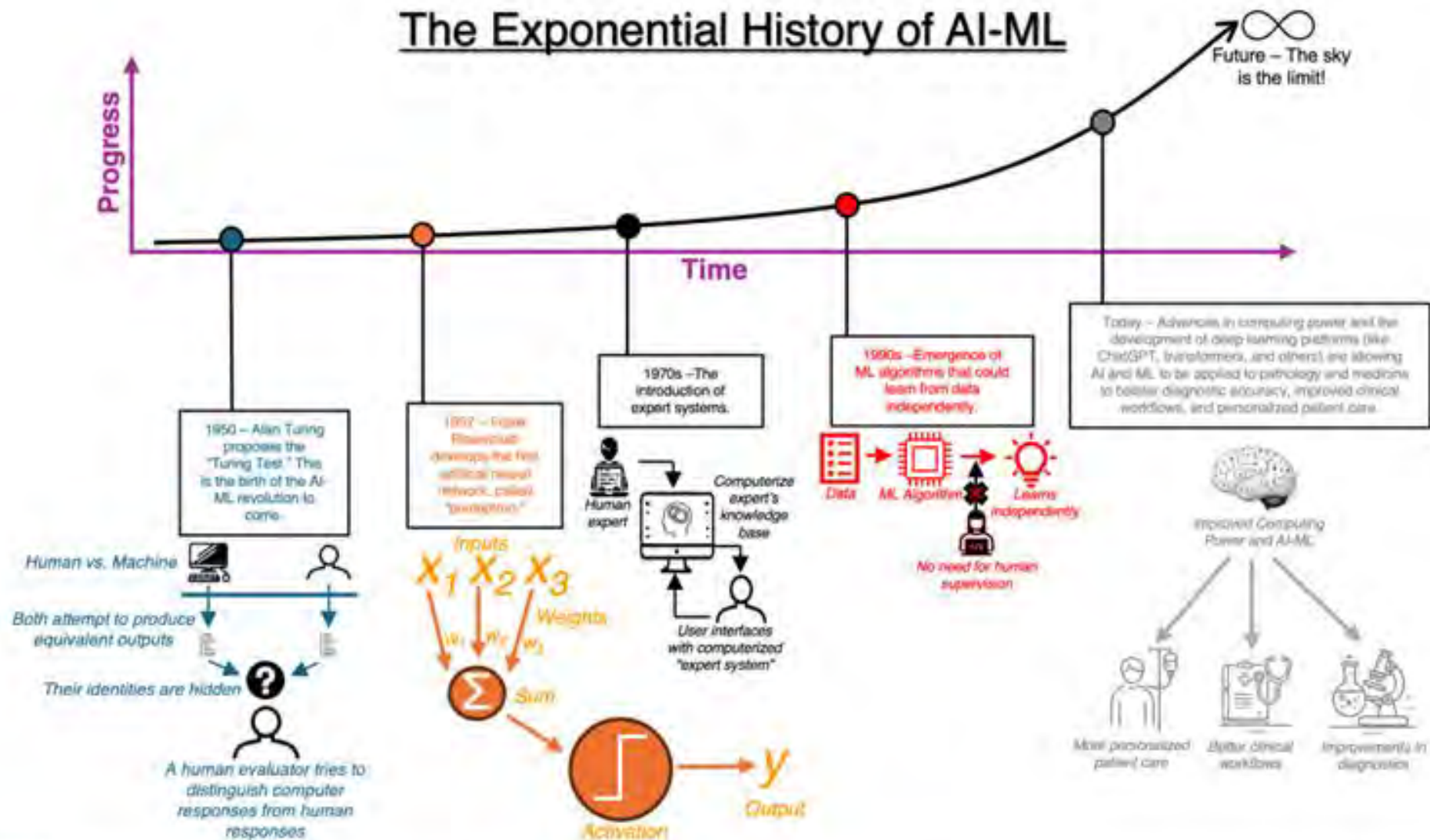
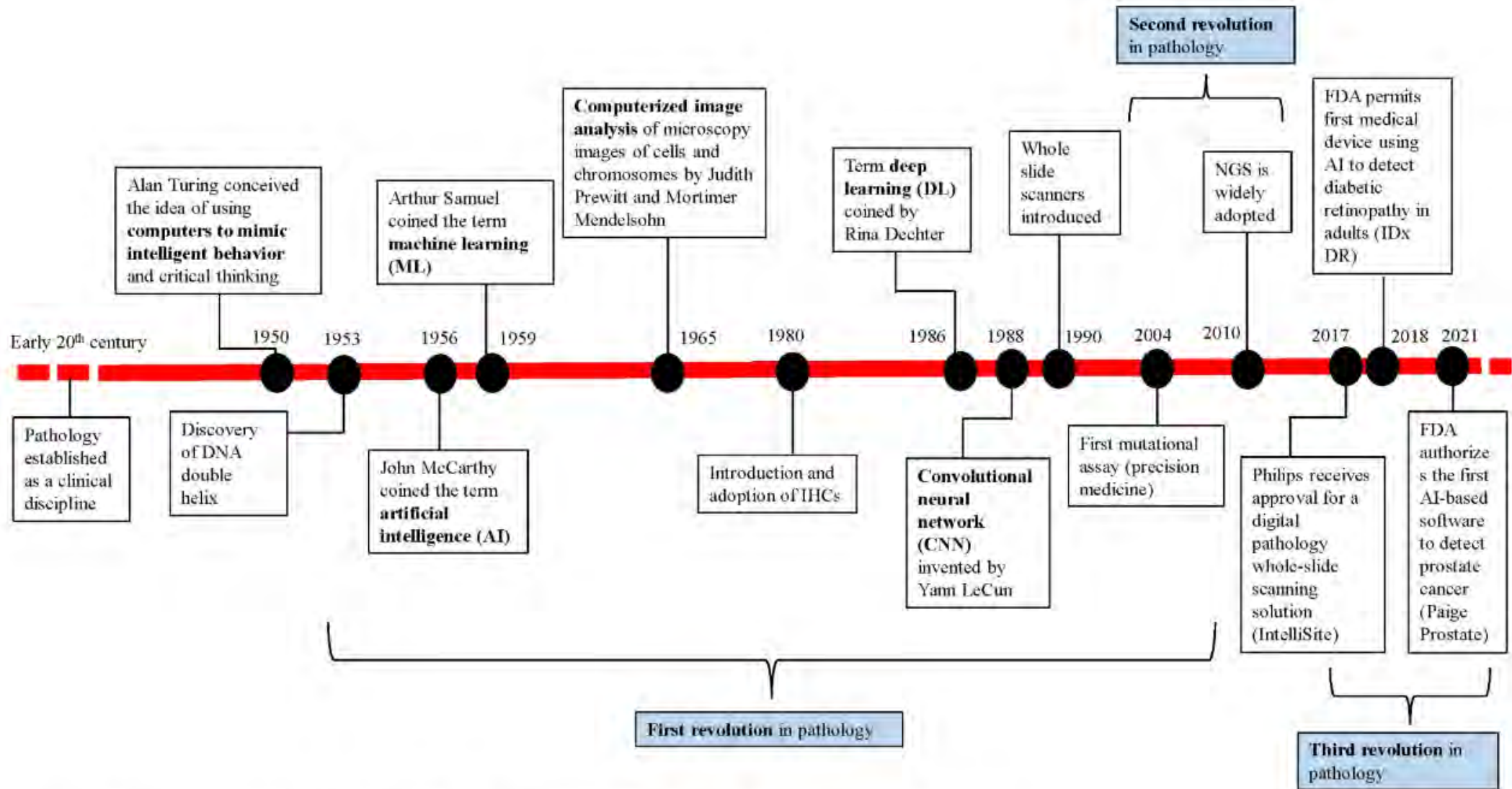


Figure 1.

Timeline of AI-ML history in pathology and medicine. All artworks were drawn by the authors in combination with generated individual embedded images via DALL-E through ChatGPT-4o. AI, artificial intelligence; GPT, generative pretrained transformer; ML, machine learning.

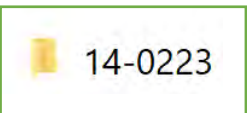


Schematic representation of the how artificial intelligence (AI) can be applied in the practice of pathology

Current Gold Standard for FPW measurement: Unbiased Stereology

Systematic Uniform Random Sampling (SURS)

Biopsy

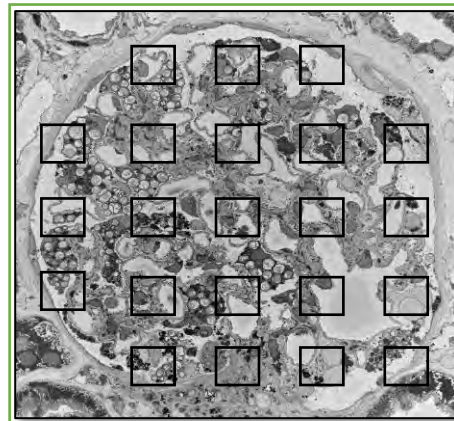


Glomeruli

- 14-0223 blk B1-1
- 14-0223 blk B1-2
- 14-0223 blk B1-3

(~3 gloms/biopsy)

SURS



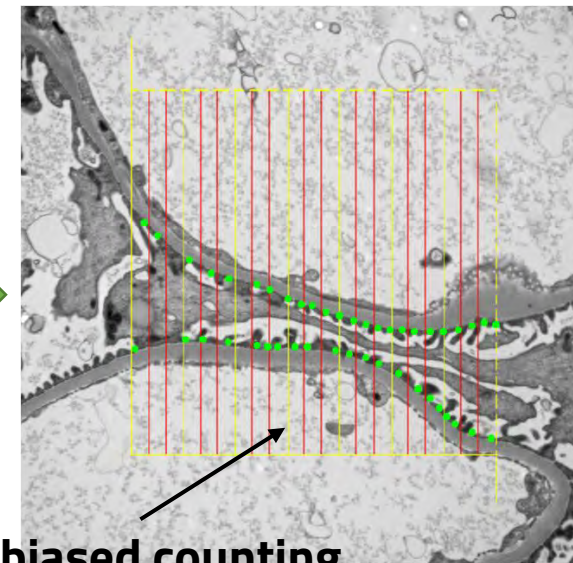
Systematic Uniform Random Sampling

SURS Images
(~30,000x mag)



(50-100 images/glom)

FPW Estimate



Unbiased counting frame

$$L_S(\text{Slit}/Z) = \frac{\sum Q_{\text{slit}}}{\sum I_{\text{intact FP}} \cdot d}$$

$$\text{FPW} = 1/L_S(\text{Slit}/Z)$$

Application of deep-learning for FPW measurement

Systematic Uniform Random Sampling (SURS)

Biopsy

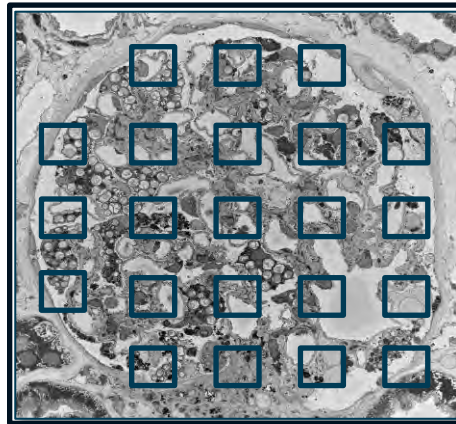
14-0223

Glomeruli

- 14-0223 blk B1-1
- 14-0223 blk B1-2
- 14-0223 blk B1-3

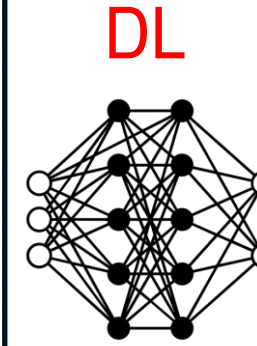
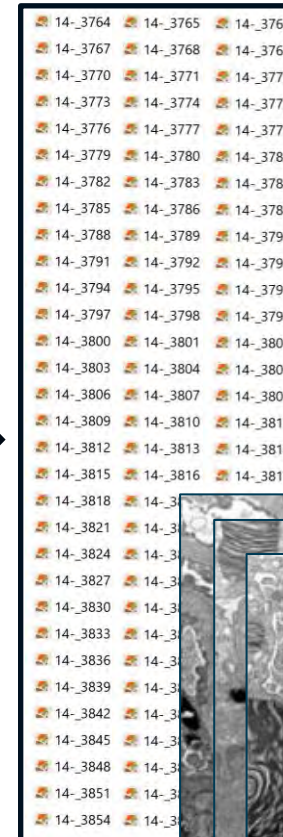
(~3 gloms/biopsy)

SURS



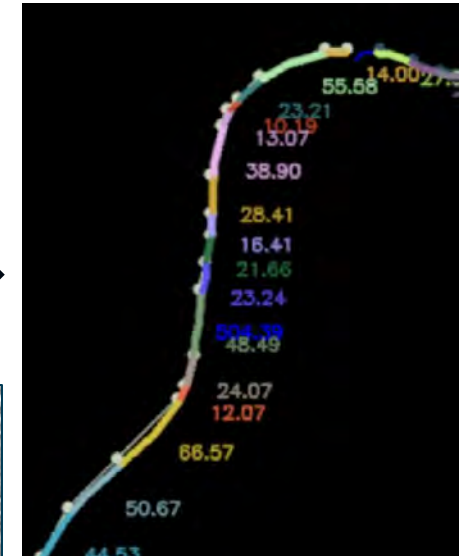
Systematic Uniform Random Sampling

SURS Images
(~30,000x)



DL

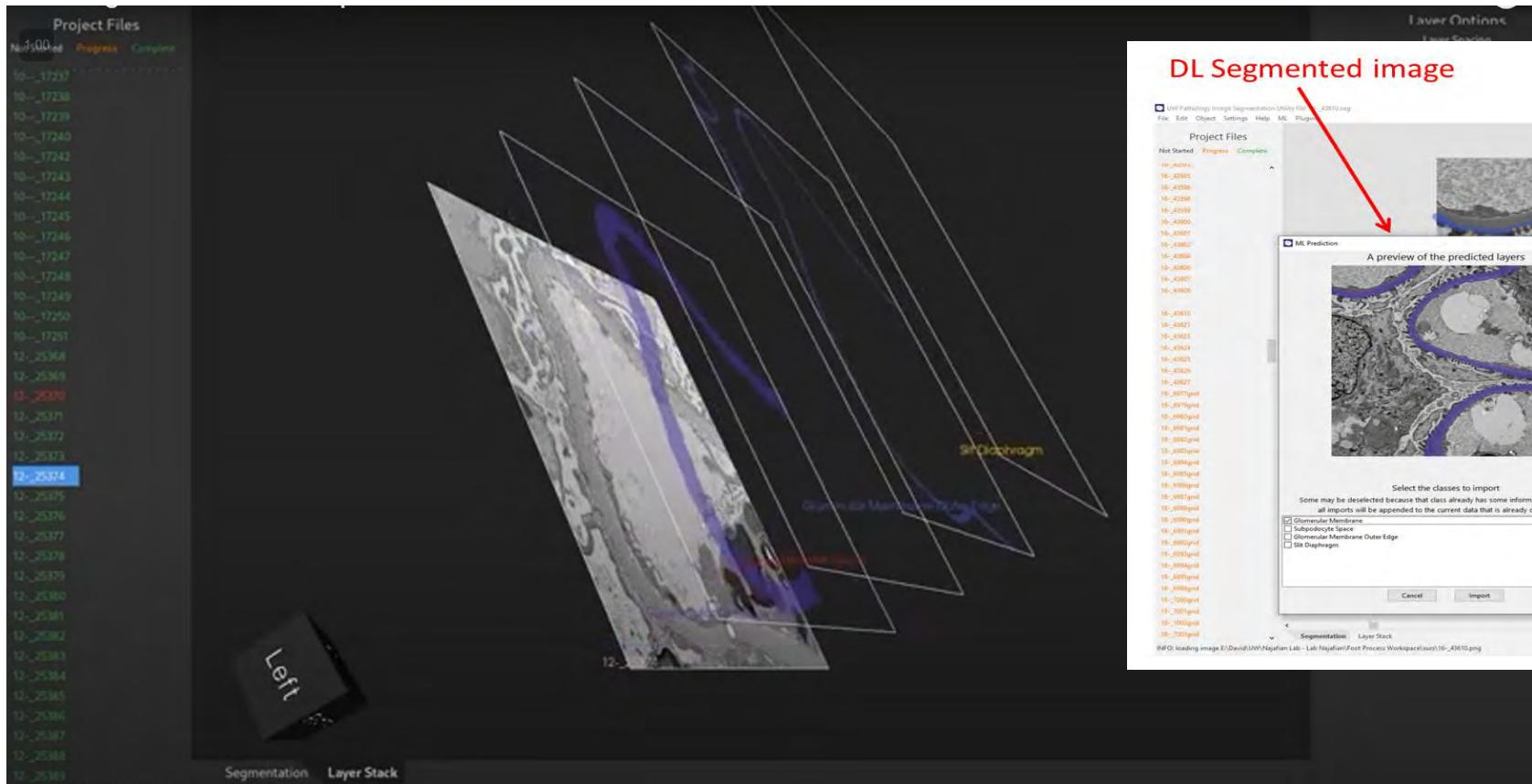
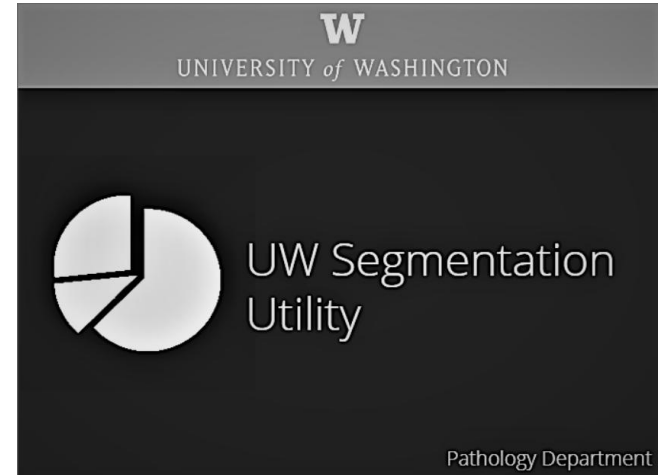
FPW



(50-100 images/glom)

Segmentation Based Dataset

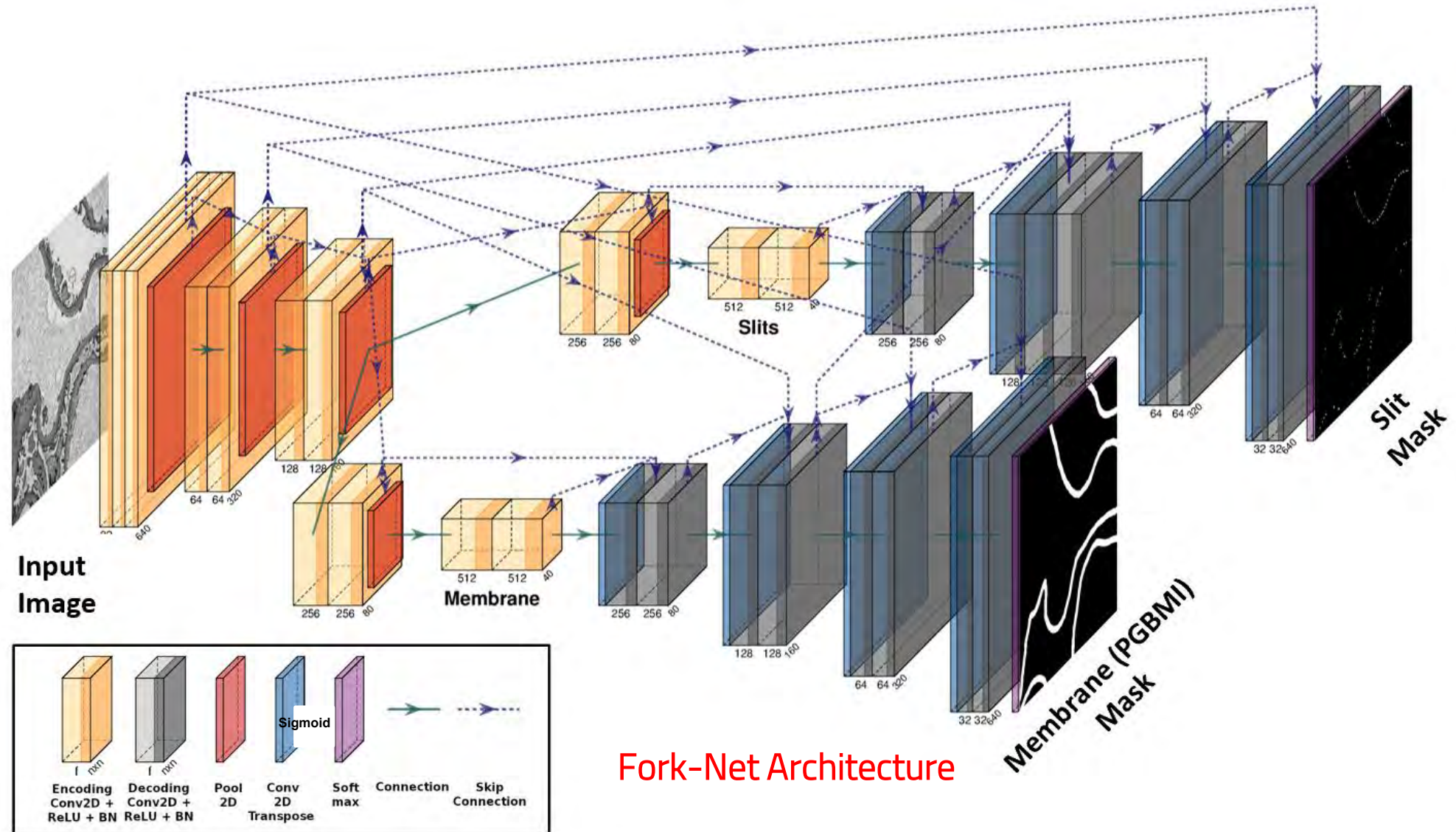
Custom Segmentation Utility with easy to use overlapping layer and multi-layer tiff support



820 GT Images, mixture of normal and diseased

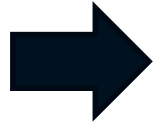
Stage 1: Convolutional Neural Network (CNN)

$Seg(I)$

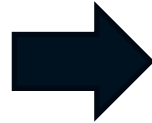
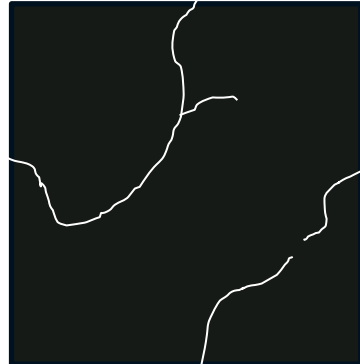


Stage 2: Computer Vision

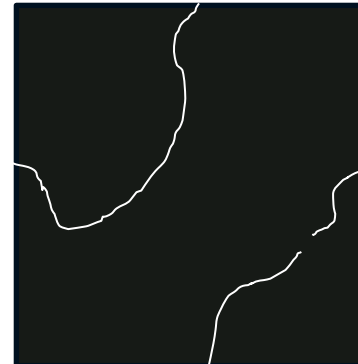
Membrane Mask



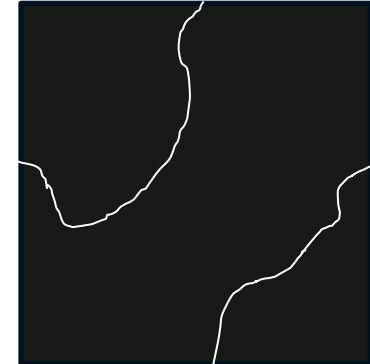
Skeletonize/
Contouring



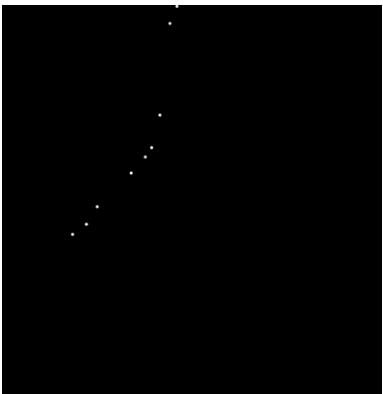
Branch/End
Identification
and Cleaning



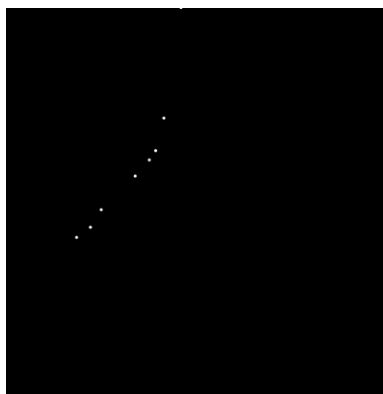
Nearby
Segment Joining



$CV(M)$
Slit Mask



Filtering and
Blob Centroid



Slit to Segment
Assignment

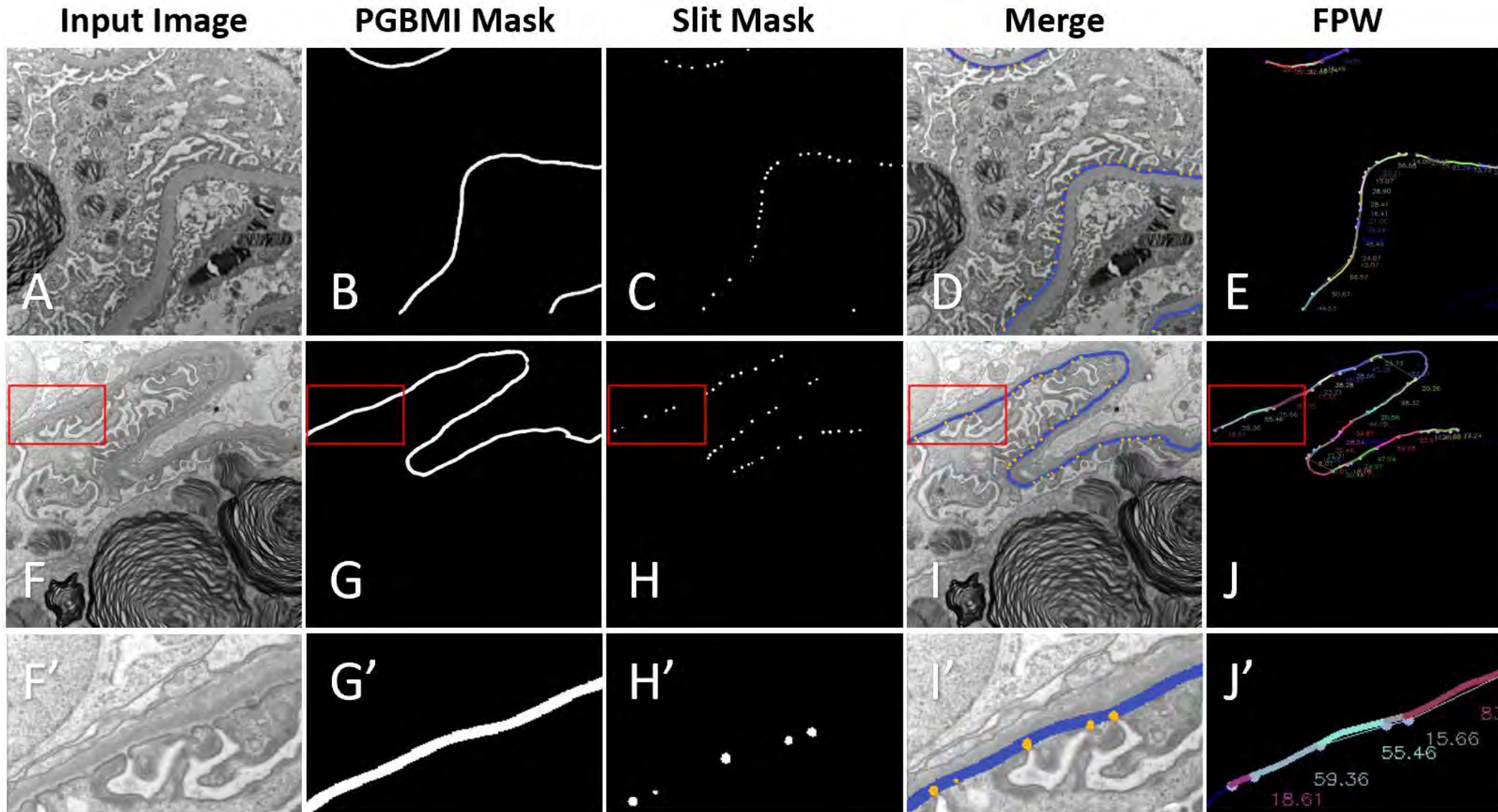


Slit Ordering/
FPW Estimation

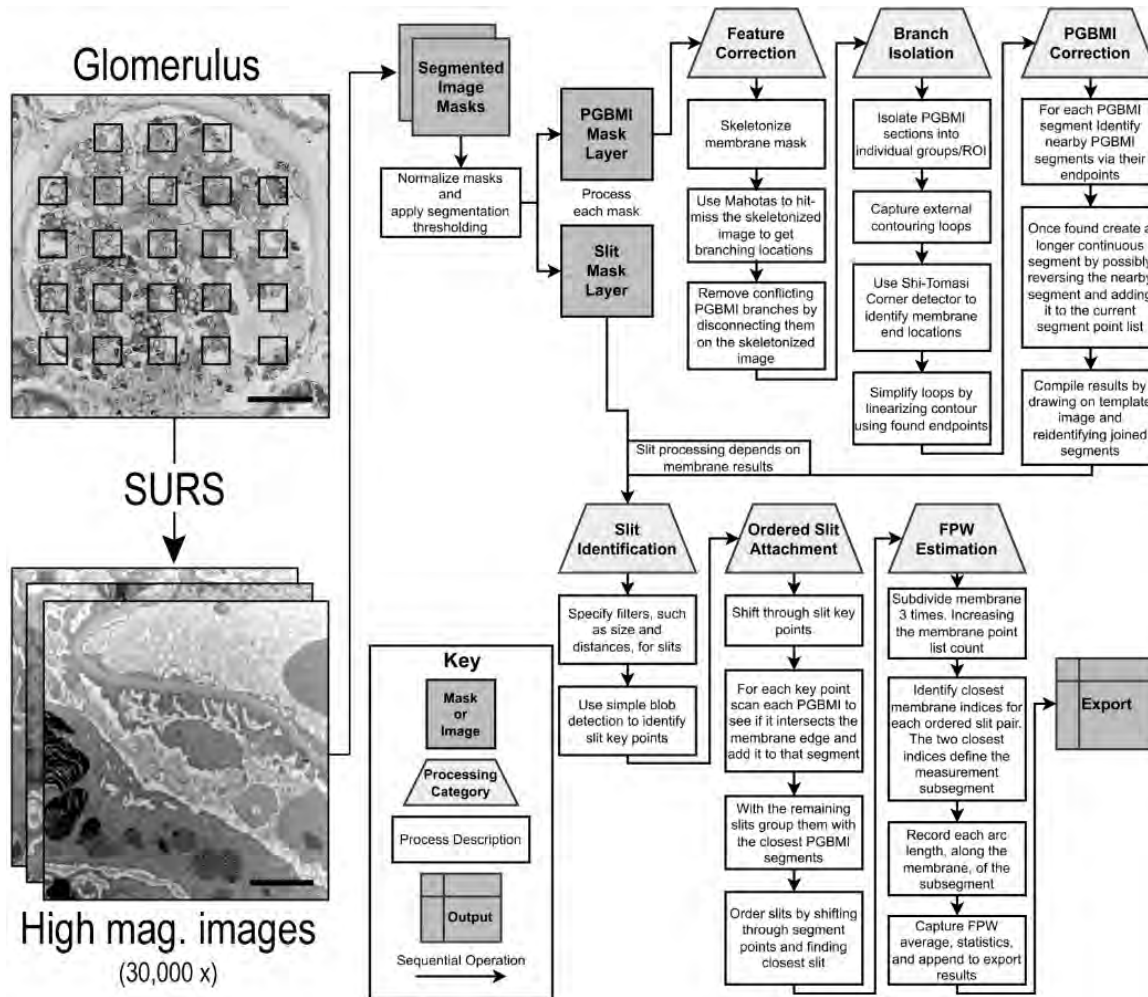


Image
Stats
 $\bar{\Delta}, \sigma^2, \dots$

Example Output



Model Workflow Diagram

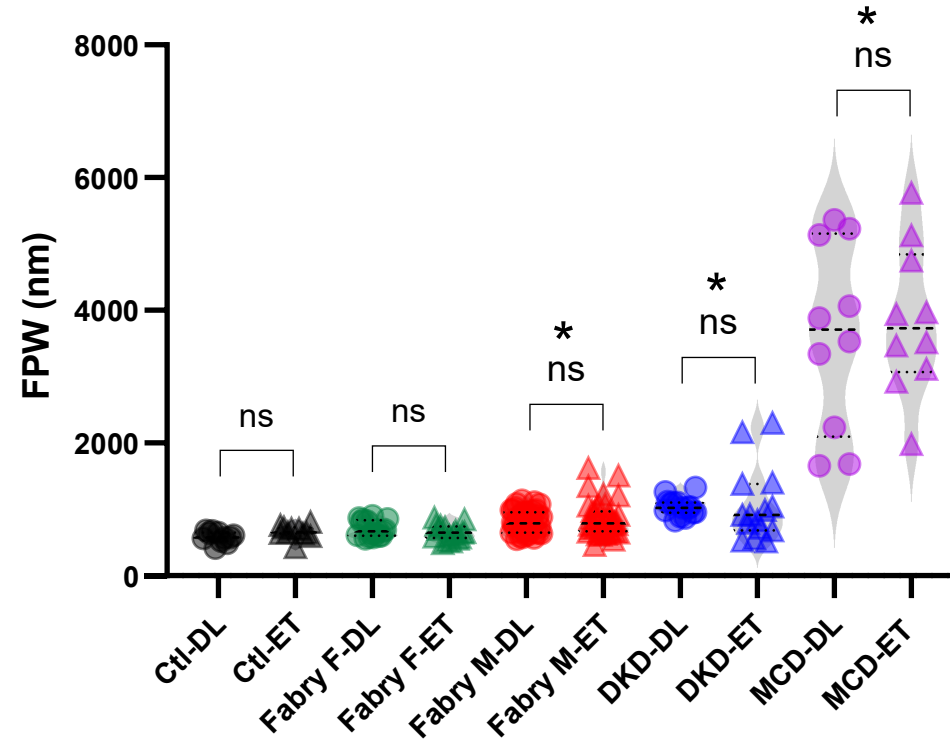


The model training accuracy measured against manual segmentation was 61-67% (15% SD) for slits and 76-86% (7.5% SD) for PGBMI.

Model precision performance on segmentation of 6960 filtration slits (i.e. positive predictive value) was 91%, with a recall (i.e. sensitivity) of 78%, and an F-score (the harmonic mean of precision and recall) of 0.84

Interchangeability of FPW Measured by Deep Learning (DL) and Expert Technician (ET)

Deep learning and human measurements were not statistically different



Ctl: control
 F: female
 M: male
 DKD: diabetic kidney disease
 MCD: minimal change disease
 ns: not significant
 *: statistically different from Ctl

Ctl (living kidney donors): n=17
 Fabry-F: n=16
 Fabry-M: n= 40
 DKD: n=15
 MCD: n=10

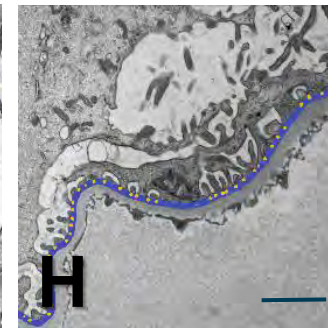
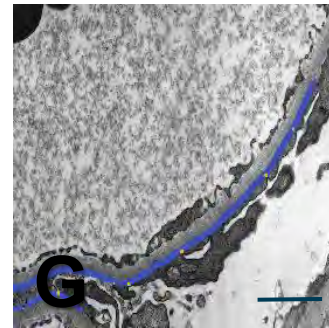
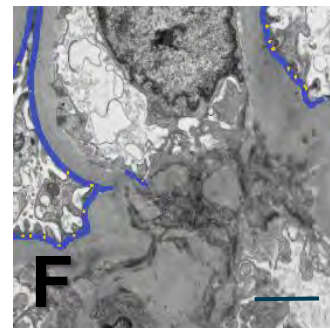
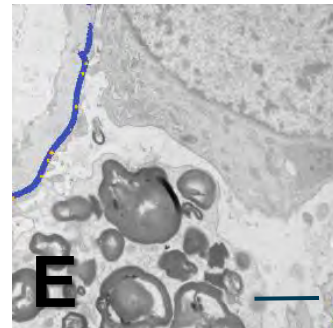
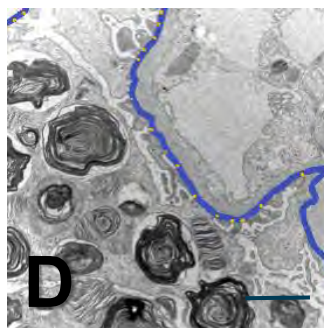
Fabry Male

Fabry Female

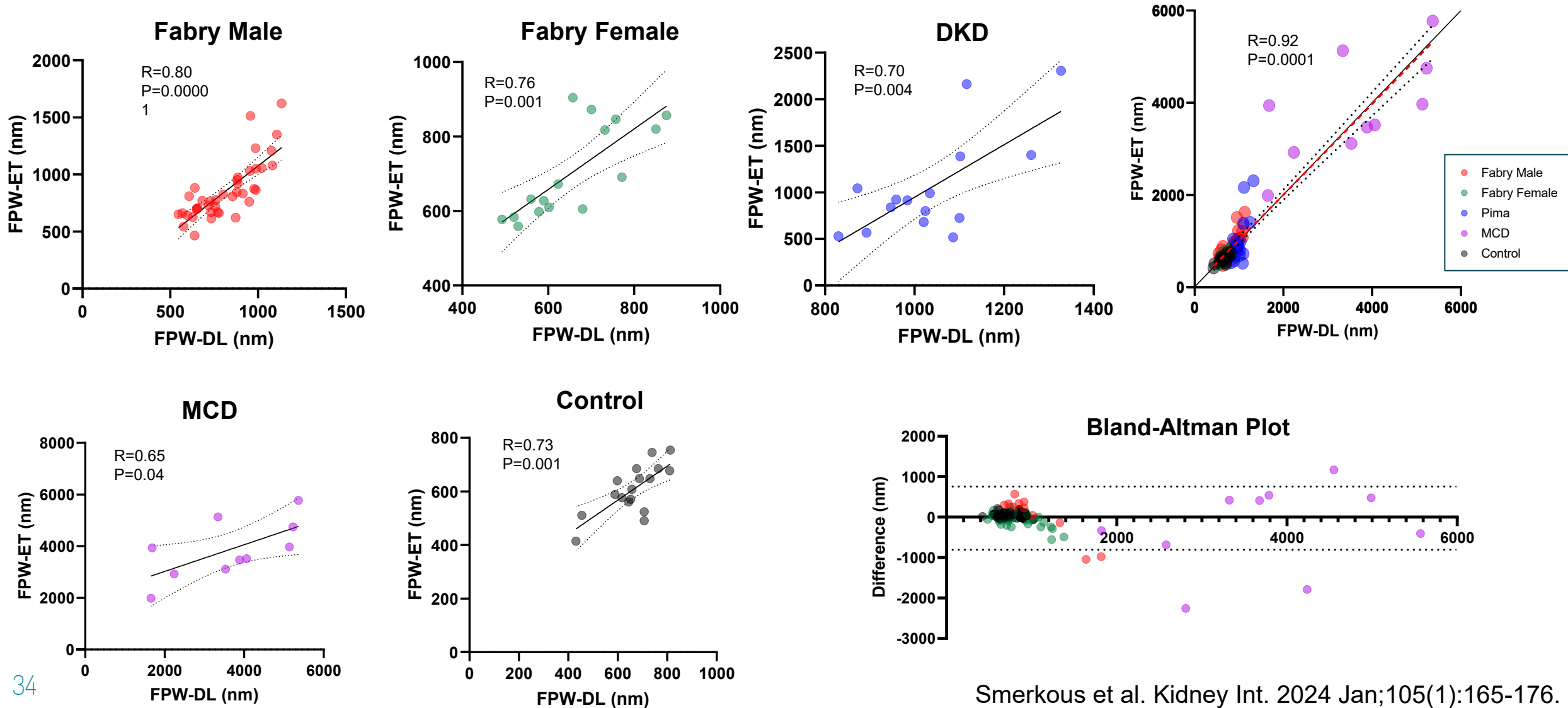
DKD

MCD

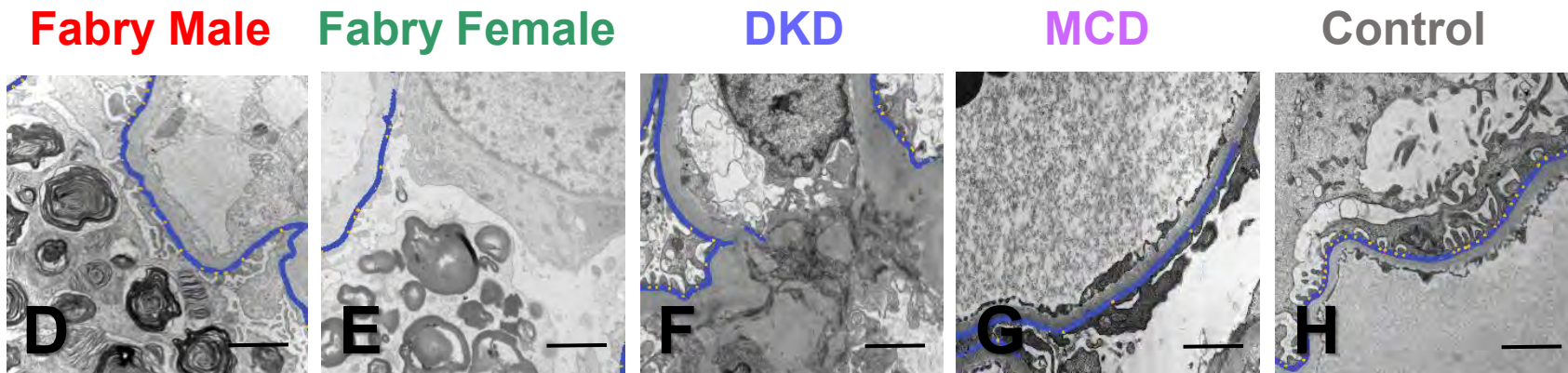
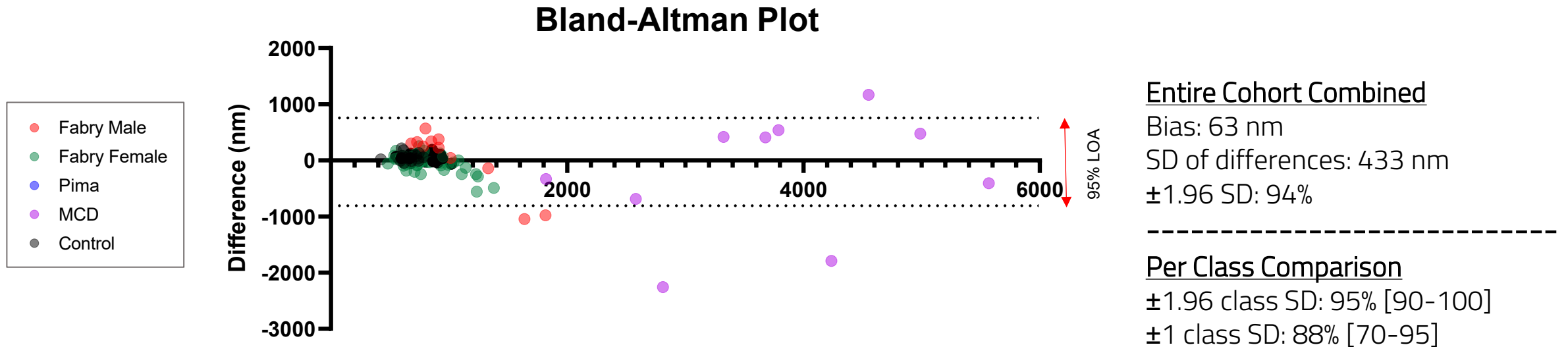
Control



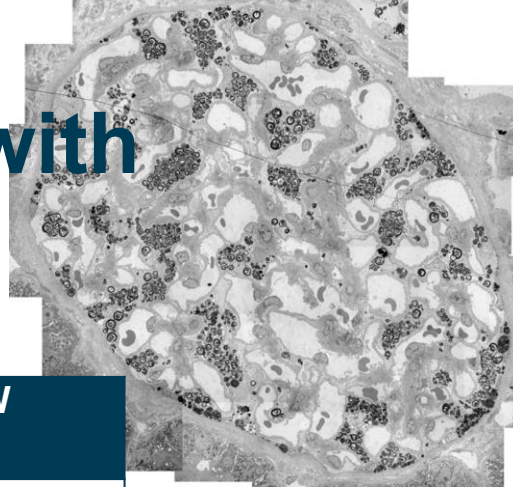
Interchangeability of FPW Measured by Deep Learning (DL) and Expert Technician (ET)



Interchangeability of FPW Measured by Deep Learning (DL) and Expert Technician (ET)



DL measurements of FPW shows Correlations with Relevant Variables – **Fabry Nephropathy**



Variable	Correlation with DL- FPW (R; p-value)	Correlation with ET-FPW (R; p-value)
Age (year)	0.40; 0.012	0.36; 0.022
UPCR	0.44; 0.005	0.58; 0.0001
% α -GAL-A activity	-0.22; 0.203	-0.29; 0.091
Plasma GL3	0.40; 0.06	0.26; 0.236
Podocyte number density ($1/\mu\text{m}^3$)	-0.44; 0.025	-0.38; 0.053
Podocyte GL3 volume fraction	0.32; 0.041	0.15; 0.349
Podocyte volume (μm^3)	0.49; 0.011	0.43; 0.028
Podocyte GL3 volume (μm^3)	0.54; 0.004	0.44; 0.026

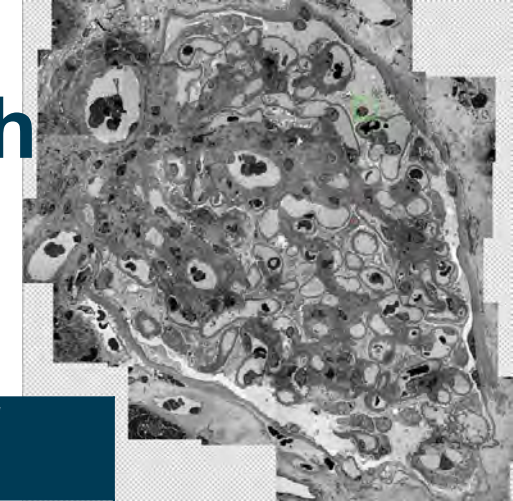
DL: deep learning

ET: expert technician

UPCR: urine protein creatinine ratio

GL3: globotriaosylceramide

DL measurements of FPW shows Correlations with Relevant Variables – **Diabetic Kidney Disease**



Variable	Correlation with DL- FPW (R; p-value)	Correlation with ET-FPW (R; p-value)
UACR	0.51; 0.05	0.30; 0.28
Mesangial fractional volume	0.61; 0.015	0.49; 0.066
Mesangial matrix fractional volume	0.62; 0.015	0.51; 0.051
Glomerular filtration surface density	-0.58; 0.024	-0.38; 0.158
GBM width (μm)	0.25; 0.376	0.36; 0.188
Podocyte volume (μm^3)	0.54; 0.037	0.37; 0.172

DL: deep learning

ET: expert technician

UACR: urine albumin creatinine ratio

GBM: glomerular basement membrane

Sources of Variability in an Experiment

$$\bar{R}_n = \frac{1}{n} \cdot \sum_{i=1}^n \hat{R}_i$$

In general:

$$OVar(\hat{R}) = Var(E[\hat{R}|R]) + E[Var(\hat{R}|R)]$$

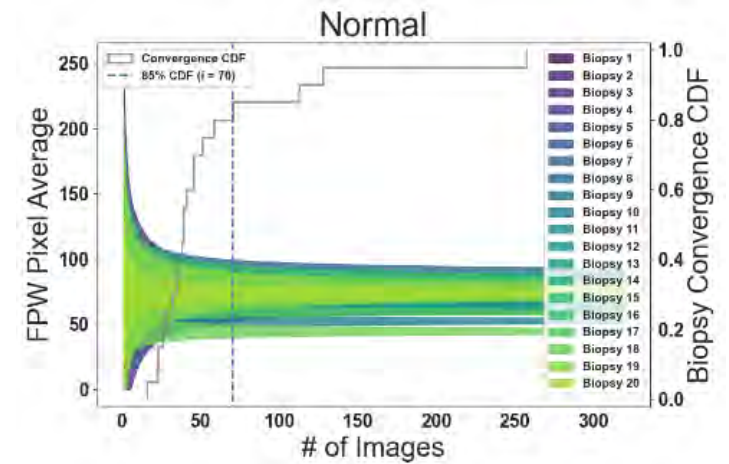
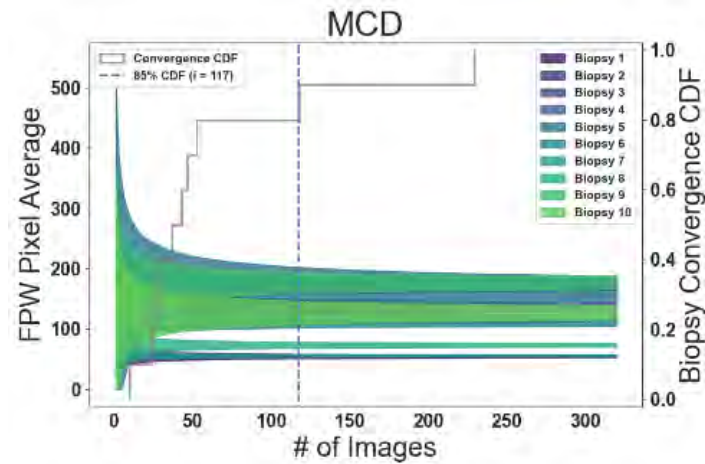
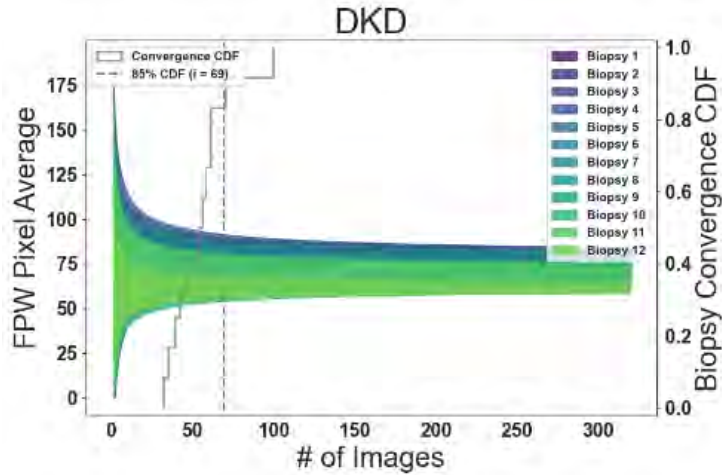
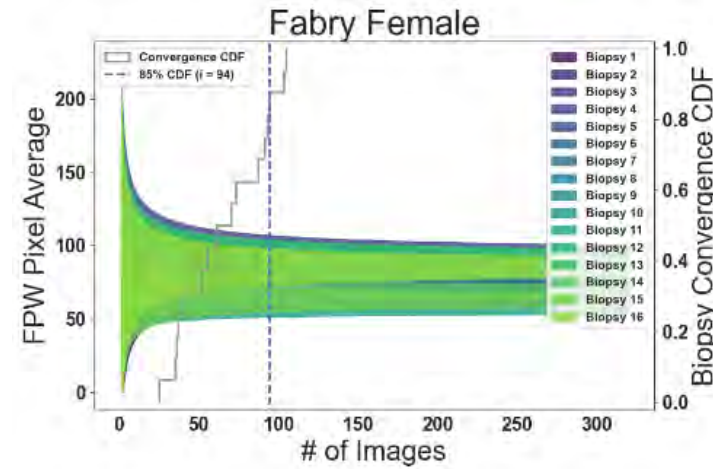
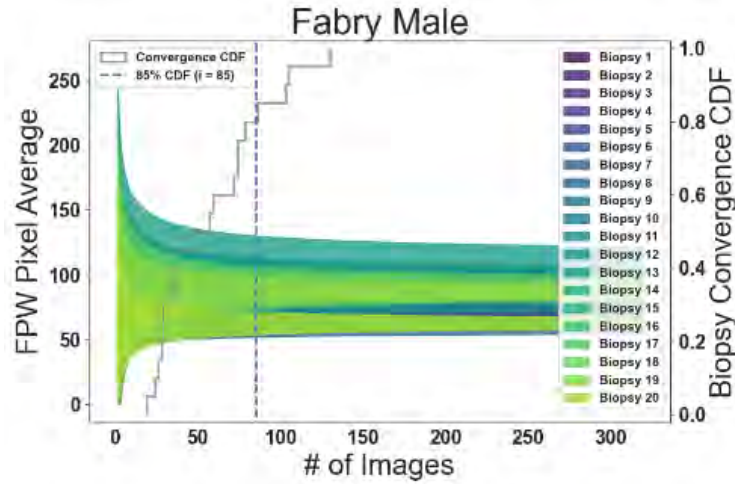
If the method of estimation is **unbiased**:

$$OVar(\hat{R}) = Var(R) + E[Var(\hat{R}|R)]$$

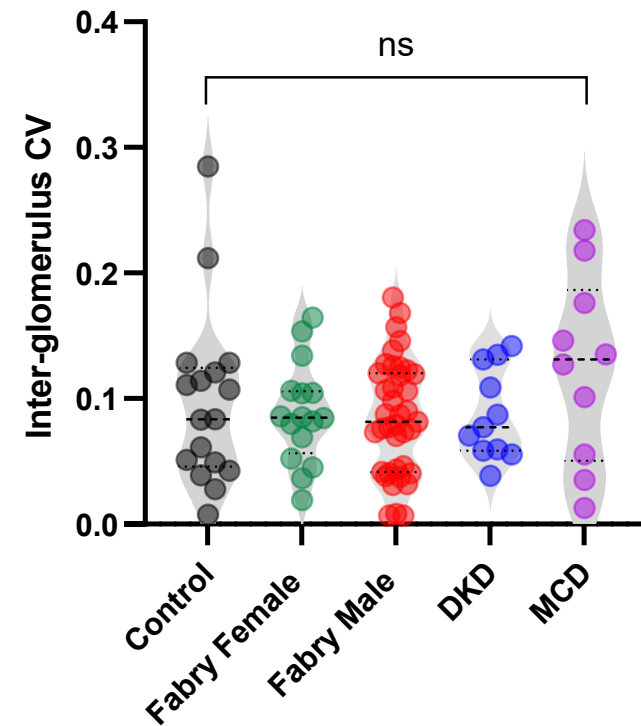
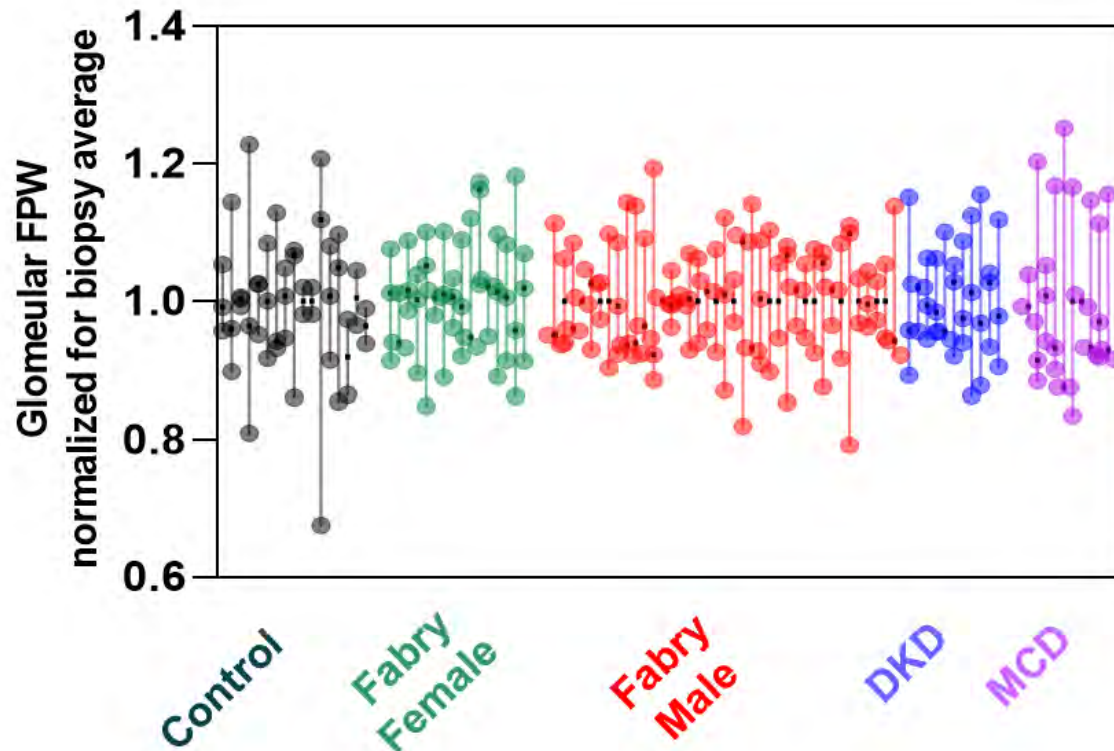
Observed Variance = Biological variation + Sampling Variance

~60 images per biopsy provided reasonably stable average FPW

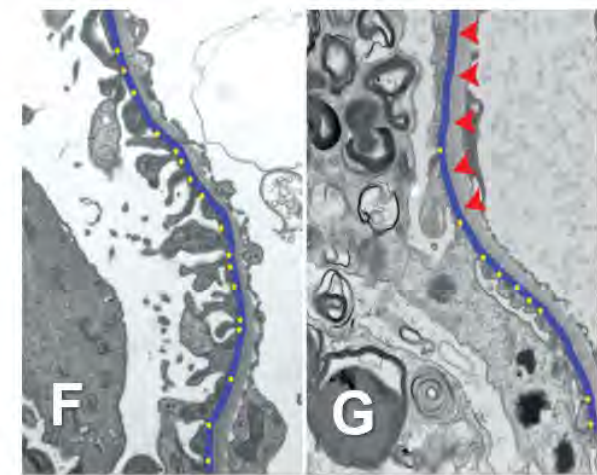
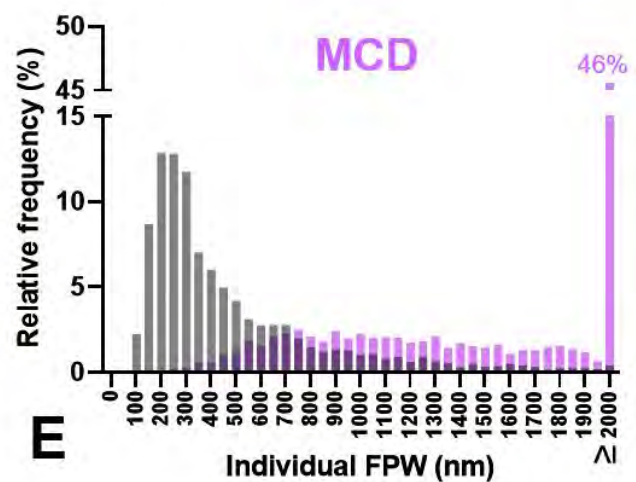
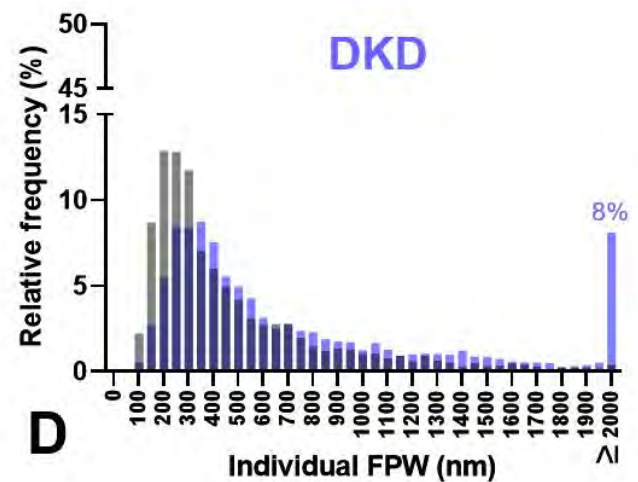
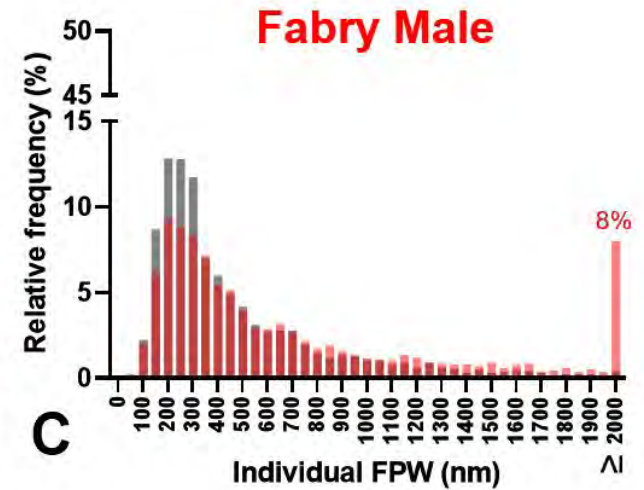
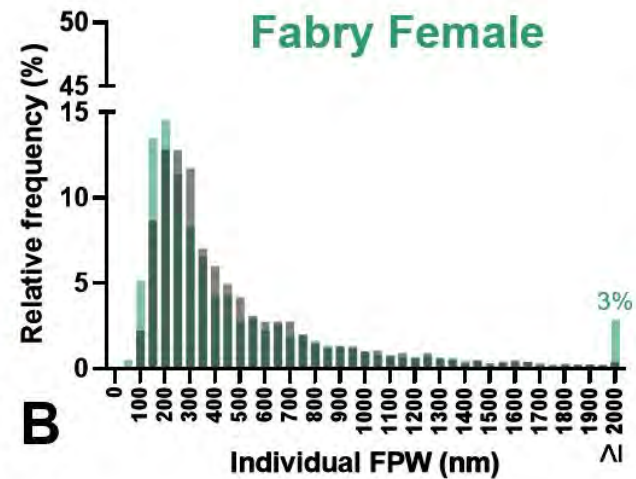
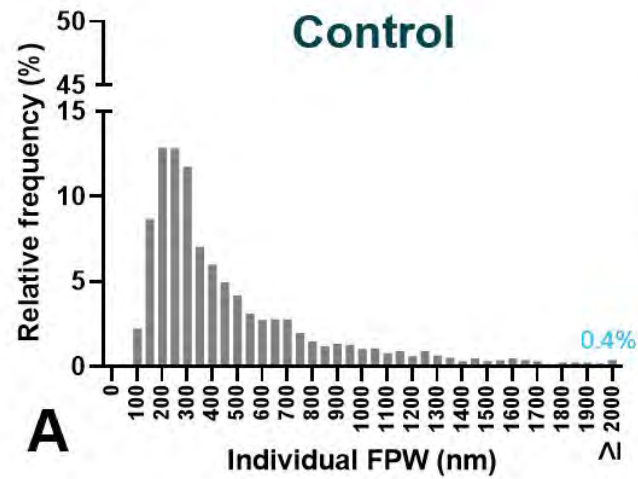
of sampled images required



Sampling Strategy: Interglomerular FPW variation?

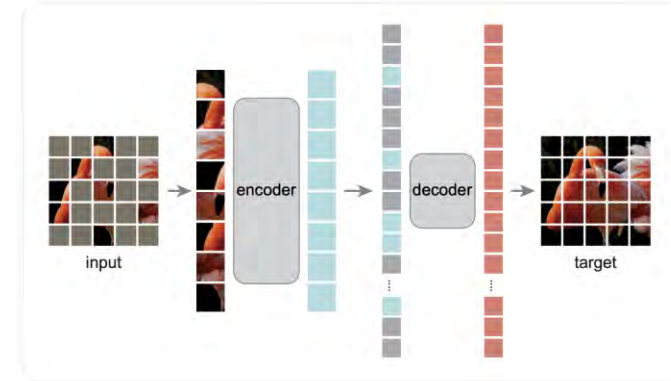


Distribution of individual FPW values: proposing a quantitative approach to segmental vs. diffuse foot process effacement



Vision Transformer – Masked Auto-Encoder (MAE)

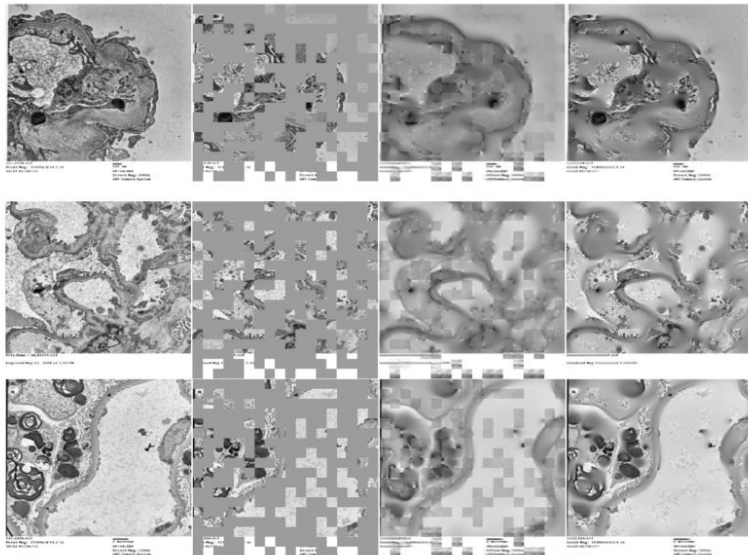
MAE (masked auto encoding) is a method for self-supervised pre-training of Vision Transformers (ViTs). The pre-training objective is that by masking a large portion (75%) of the image patches, the model must reconstruct raw pixel values.



He et al. arXiv:2111.06377v3 [cs.CV] 19 Dec 2021

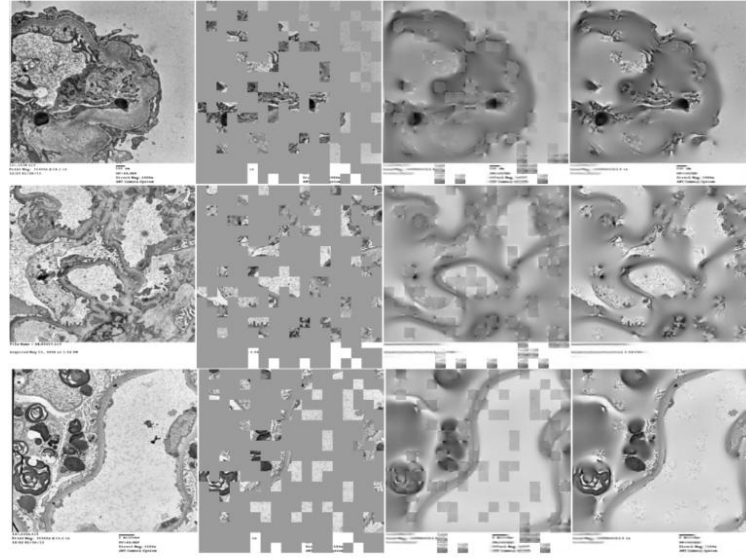
65% of Image Masked

Input masked predicted merged



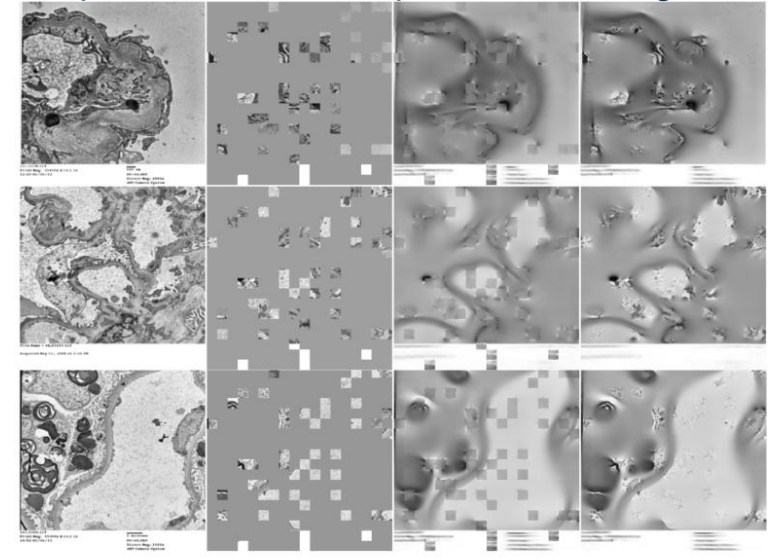
75% of Image Masked

Input masked predicted merged



85% of Image Masked

Input masked predicted merged



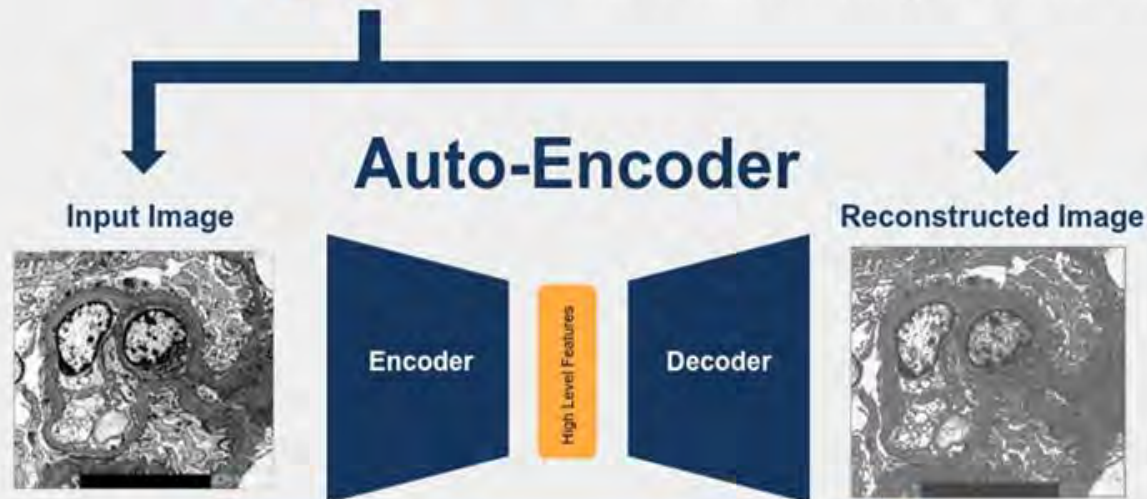
Model Implementation

Pre-training (self-supervised)

190,000 EM images



Train an auto-encoder to “compress” high-dimensional image into a lower dimensional space, and decompress images back to the original image. Forcing model to learn semantically meaningful classes and geometry for reconstruction.



Project to lower dimensional representation and reproject to image space

Use model from pre-training as starting point for supervised model

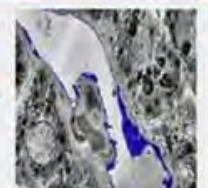
Supervised Training



High Level Features



Expert Labeled

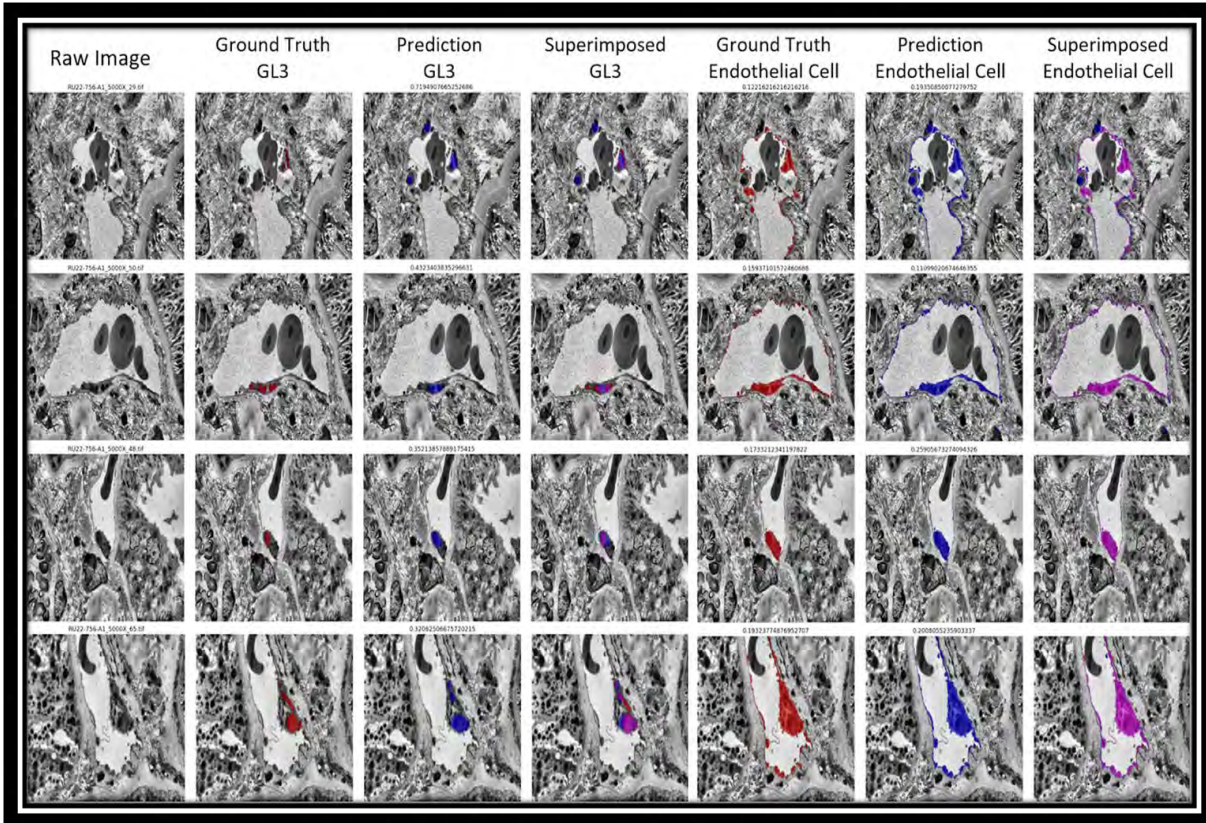


Predicted

Use expert-labeled images to guide segmentation model



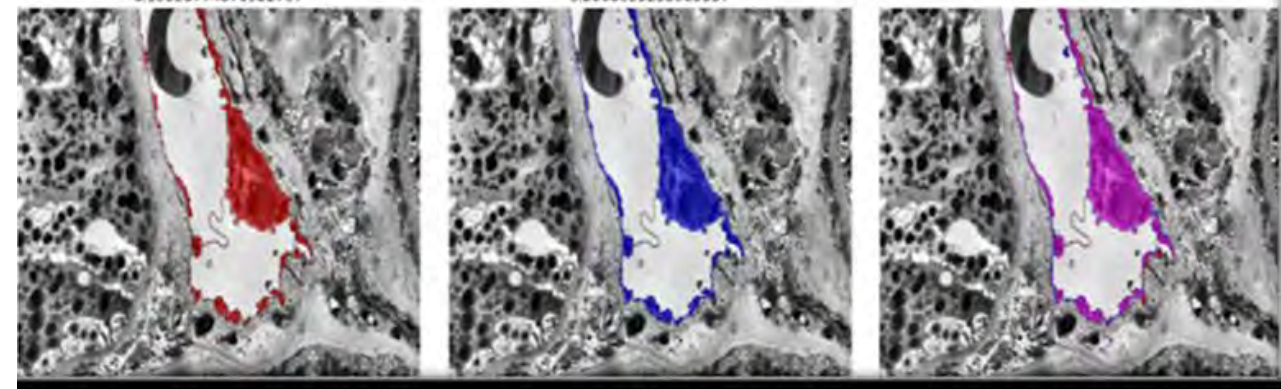
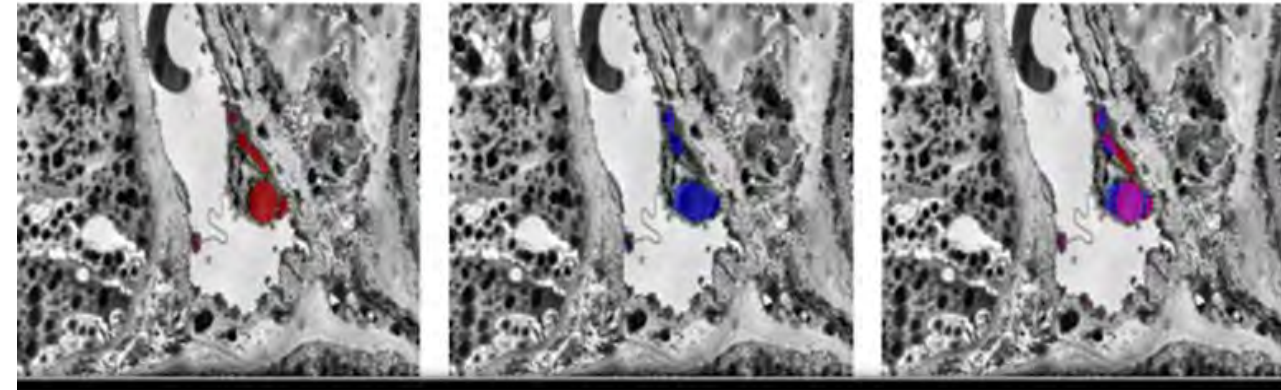
Results



Ground Truth
GL3(top)/EC(bottom)

Predicted

Superimposed



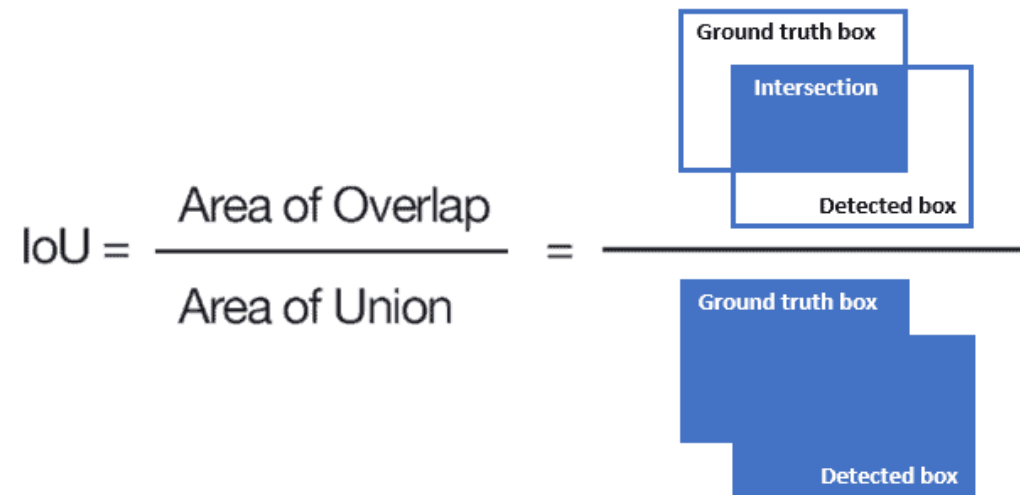
$$Vv(Inc/Endo_{PTC}) = \frac{\sum_{i=0}^n A_{GL3}}{\sum_{i=0}^n A_{Endo} - \sum_{i=0}^n A_{nuc}}$$

$Vv(Inc/Endo_{PTC})$ = fraction of endothelial cells occupied by GL3 inclusions; A = area (pixel); PTC = peritubular capillary



Results

Measurement	All Images (Train + Test)	Train (Fabry + Normal)	Train (Fabry)	Train (Normal)	Test (Fabry + Normal)	Test (Fabry)	Test (Normal)	
GL3 IOU \pm STD	0.8263 \pm 0.2895	0.8249 \pm 0.2957	0.6153 \pm 0.3390	0.9962 \pm 0.0000	0.8382 \pm 0.2346	★	0.6101 \pm 0.2131	0.9962 \pm 0.0000
EC IOU \pm STD	0.8162 \pm 0.1118	0.8179 \pm 0.1153	0.8264 \pm 0.0750	0.8110 \pm 0.1399	0.8020 \pm 0.0747	★	0.8613 \pm 0.0507	0.7610 \pm 0.0601
Nucleus IOU \pm STD	0.8401 \pm 0.2521	0.8364 \pm 0.2628	0.8850 \pm 0.1914	0.7967 \pm 0.3044	0.8716 \pm 0.1276	★	0.8267 \pm 0.1578	0.9027 \pm 0.0965
GL3 Inc Ratio Ground Truth	0.0431 \pm 0.0916	0.0415 \pm 0.0916	0.0922 \pm 0.1185	0.0000 \pm 0.0000	0.0574 \pm 0.0922	★	0.1403 \pm 0.0962	0.0000 \pm 0.0000
GL3 Inc Ratio Model Predicted	0.0478 \pm 0.1001	0.0437 \pm 0.0933	0.0972 \pm 0.1193	0.0000 \pm 0.0000	0.0833 \pm 0.1438	★	0.2035 \pm 0.1635	0.0000 \pm 0.0000
Absolute Error	0.0168 \pm 0.0428	0.0152 \pm 0.0382	0.0338 \pm 0.0513	0.0000 \pm 0.0000	0.0309 \pm 0.0705		0.0755 \pm 0.0962	0.0000 \pm 0.0000

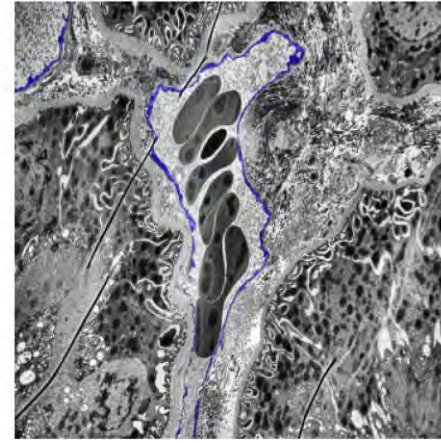
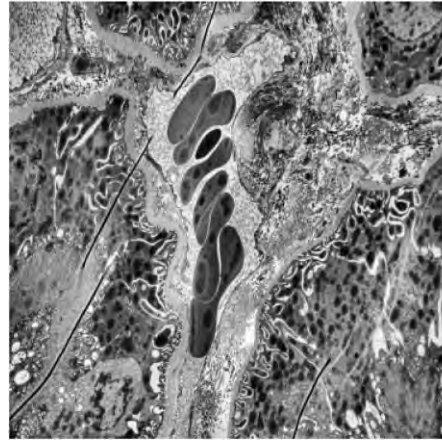
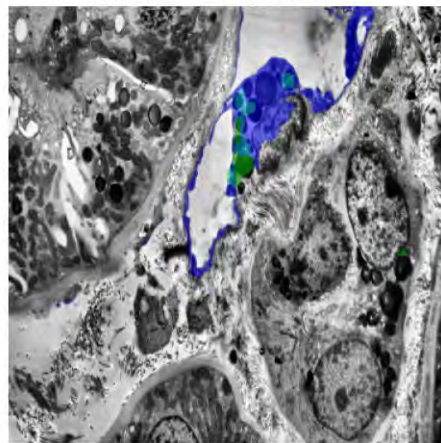
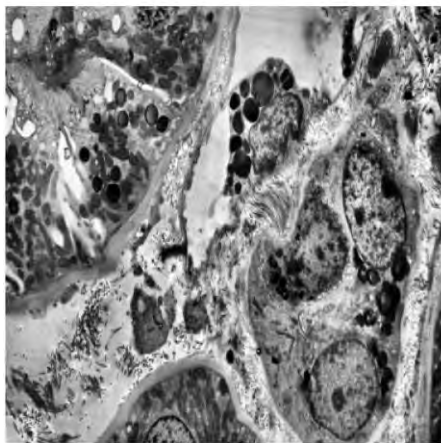
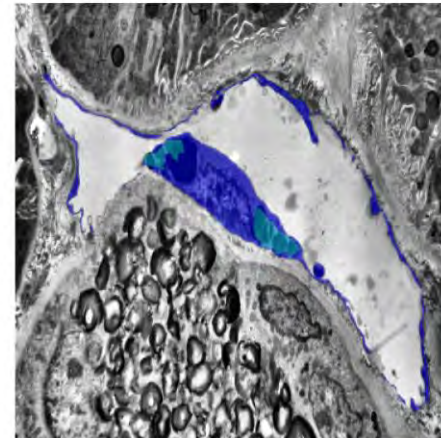
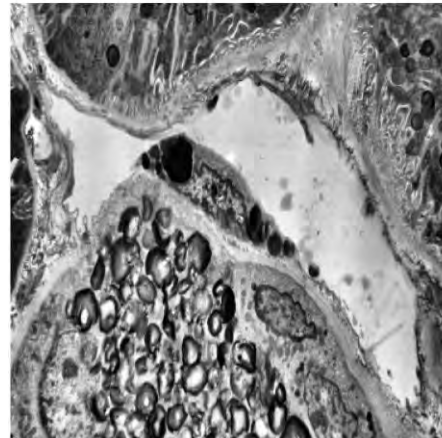
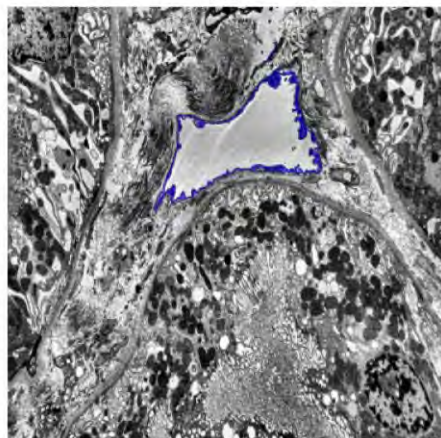
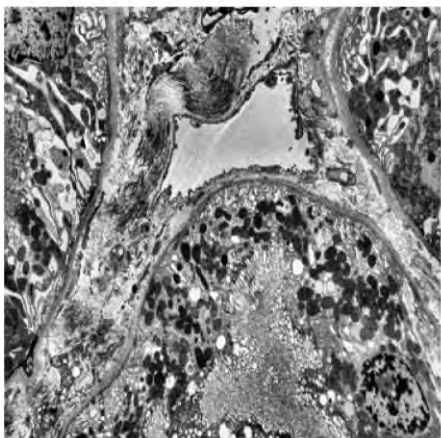
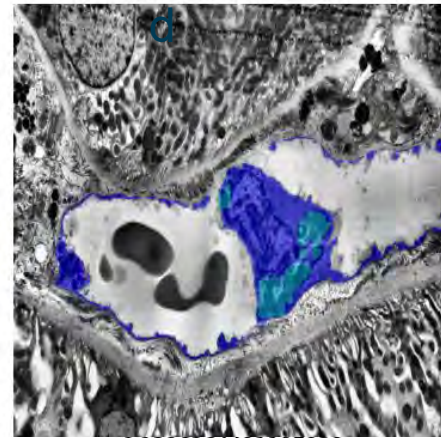
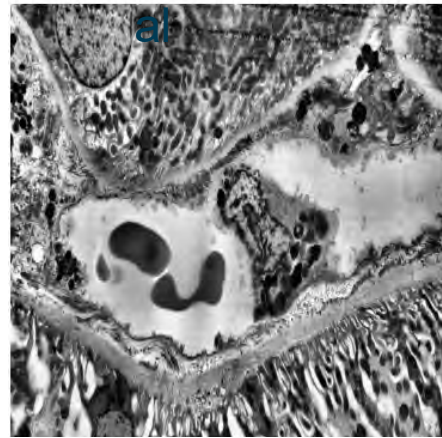
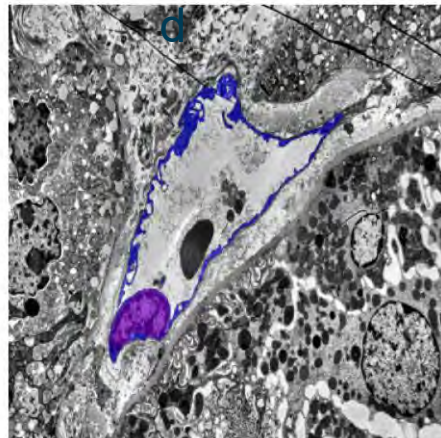
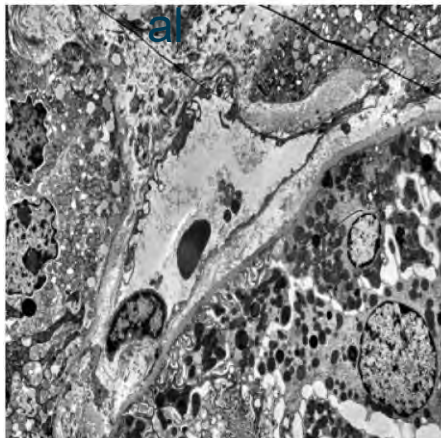


Origin

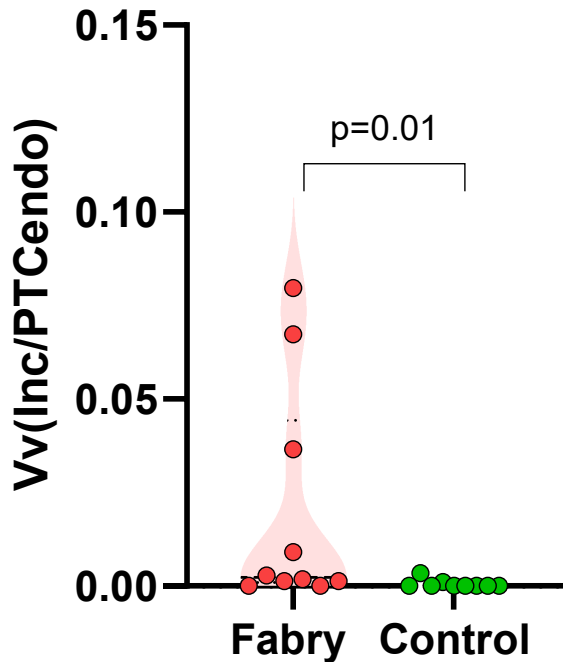
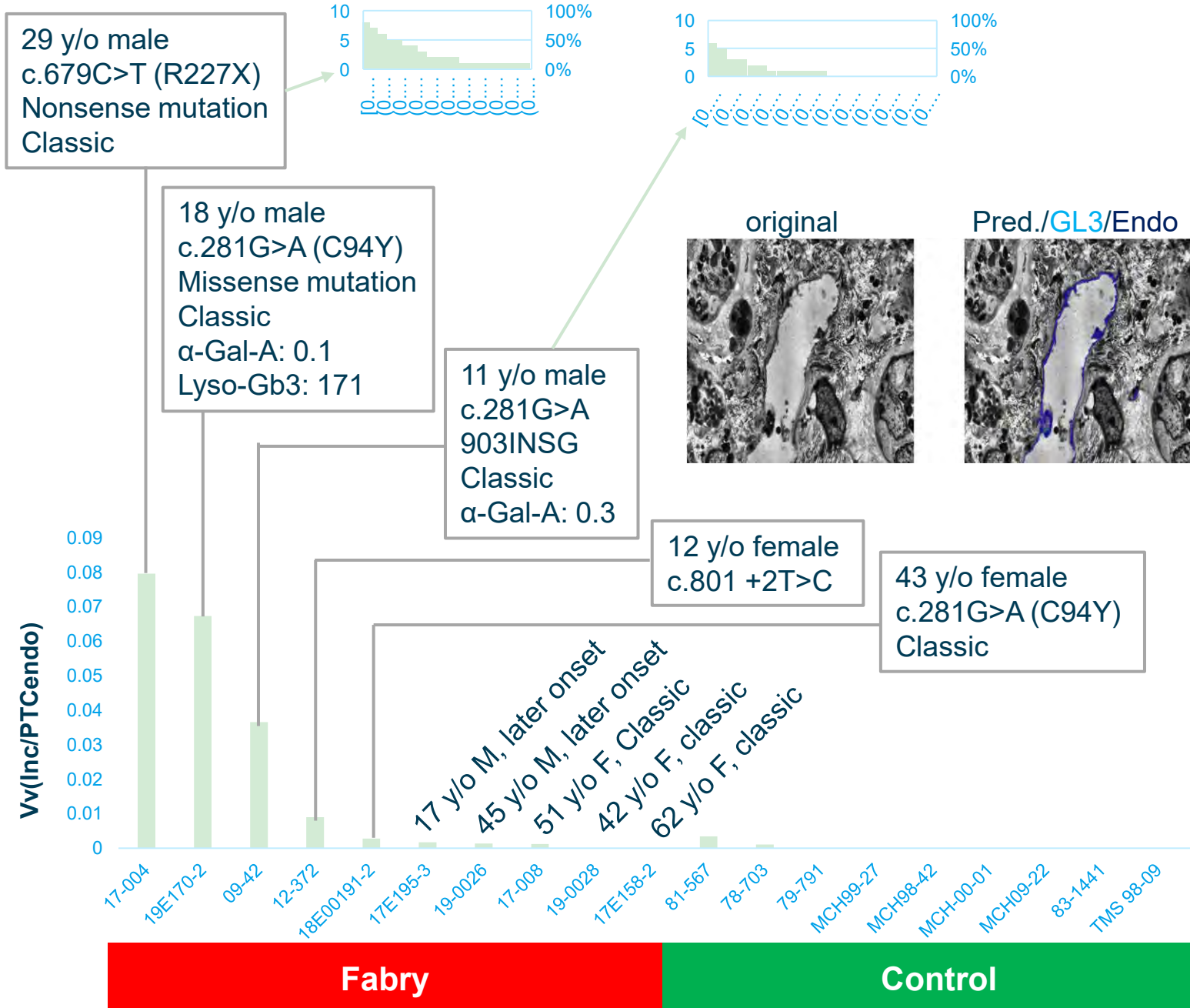
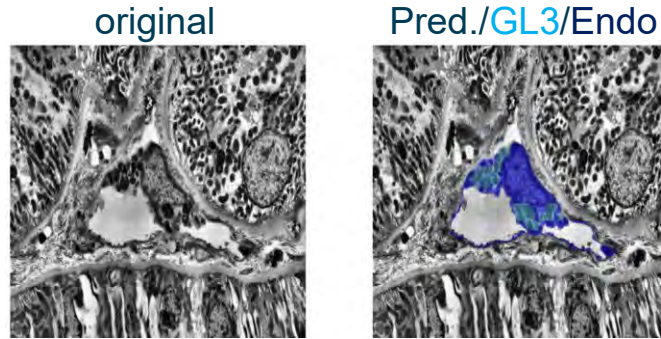
Predicted

Origin

Predicted

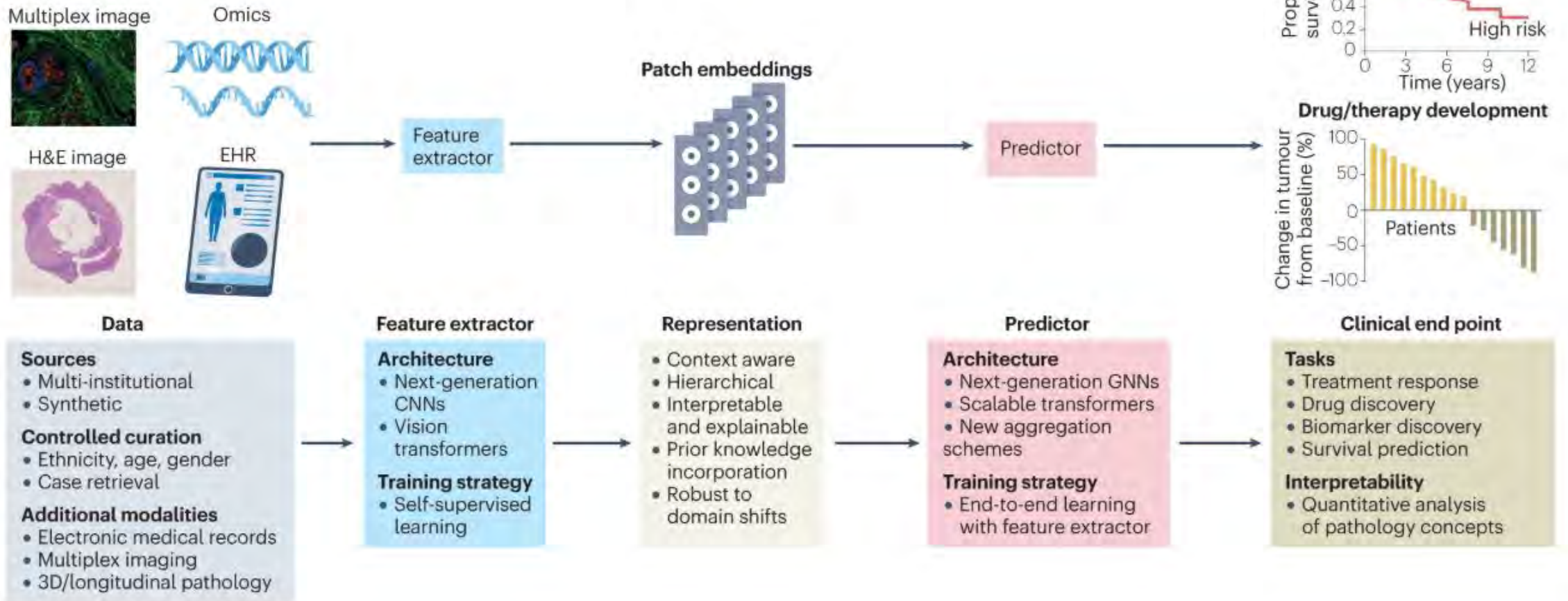


Peritubular Capillary Endothelial GL3 Inclusion Fractional Volume [Vv(Inc/PTCendo)]



Future directions in computational pathology

a Future directions



Roadblocks and challenges preventing AI application

- **Ethical principles and AI**
- **Validation of algorithms and overfitting**
- **Interpretability and the ‘black box’ problem**
- **Quality of data**
- **Computational system, data storage and cost-benefit ratio**
- **Technological issues**
- **Regulation, reimbursement, and clinical adoption**
- **Pathologists’ dilemma-to use or not to use**

Conclusions

- There has been a tremendous growth in the development of novel AI approaches in pathology in the last few years.
- AI can improve diagnostic workflows, eliminate human errors, increase inter-observer reproducibility, and make prognostic predictions.
- While there has been an increase in the development of AI tools, the integration into clinical practice has somewhat lagged owing to several issues related to interpretability, validation, regulation, generalizability, and cost.

Acknowledgement

Najafian Lab, University of Washington



David Smerkous



Andy Wang



Alex Amedson



Kimia Tork



Ahmet Yazlyyev



Samantha Goorin



Ben Katznelson



Nikki Hasibi



Reza Hosseini



Alireza Ayoubi



Frank Dastvan



Josh Russel

Our Collaborators



Michael Mauer, M.D.
Pediatric Nephrology
University of Minnesota



Sheng Wang, Ph.D
Computer Science & Engineering
University of Washington

All Collaborators who provided biopsies:

E. Svarstad, C. Tøndel, D. Warnock, S. Waldek, M.C. Gubler, M. West, JP. Oliveira, J. Geng, M. West

Funding

These studies were sponsored by grants from NIH/NCATS U54NS065768, NIDDK/Diabetes Complication Consortium U24 DK128851, 1R03HD111661-01 (NIH/NICHHD), and investigator initiated grants from Sanofi and Amicus Therapeutics, Sanofi Rare Genetic Disease Focused Fellowship SGZ-2023-23999.

THANK YOU!

Program Evaluation and CE Credit

- We need your assistance. Your opinion is important.
- Please go to the link below and help us evaluate the program. You can
 - also claim continuing education credit at this link.
- ldrctc.cds.affinityced.com